



Universiteit Leiden

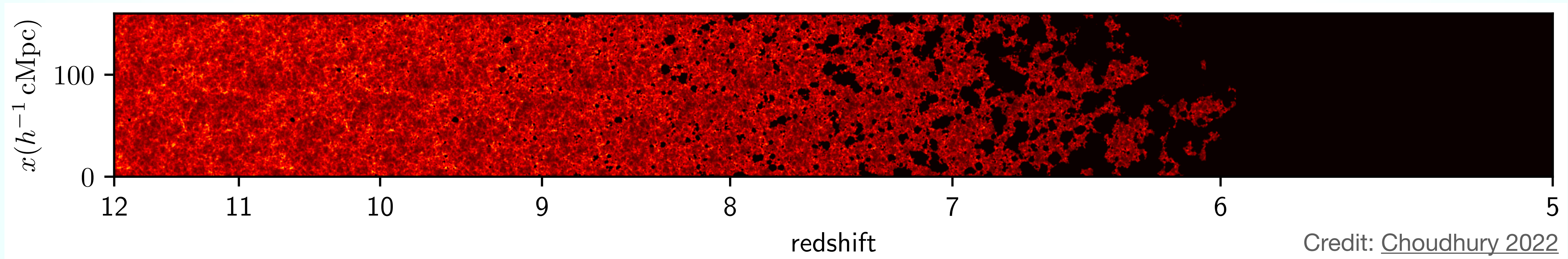


Constraining the Reionization History with High- z Quasar Damping Wings

Timo Kist, PhD candidate at Leiden Observatory
Supervisor: Joseph F. Hennawi

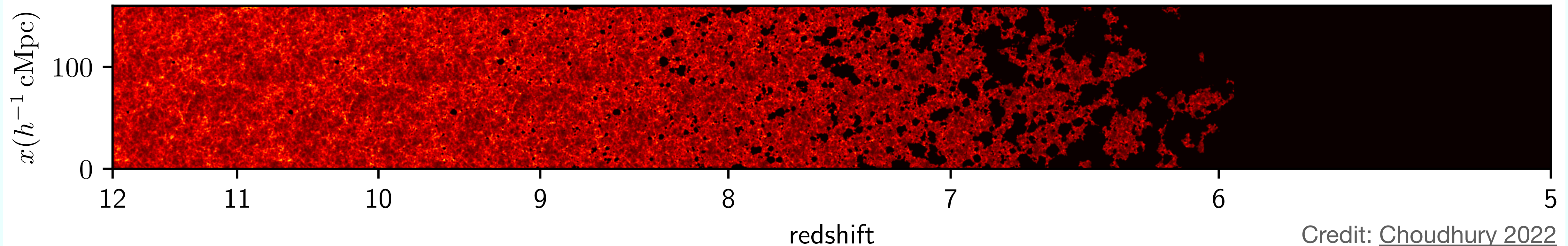
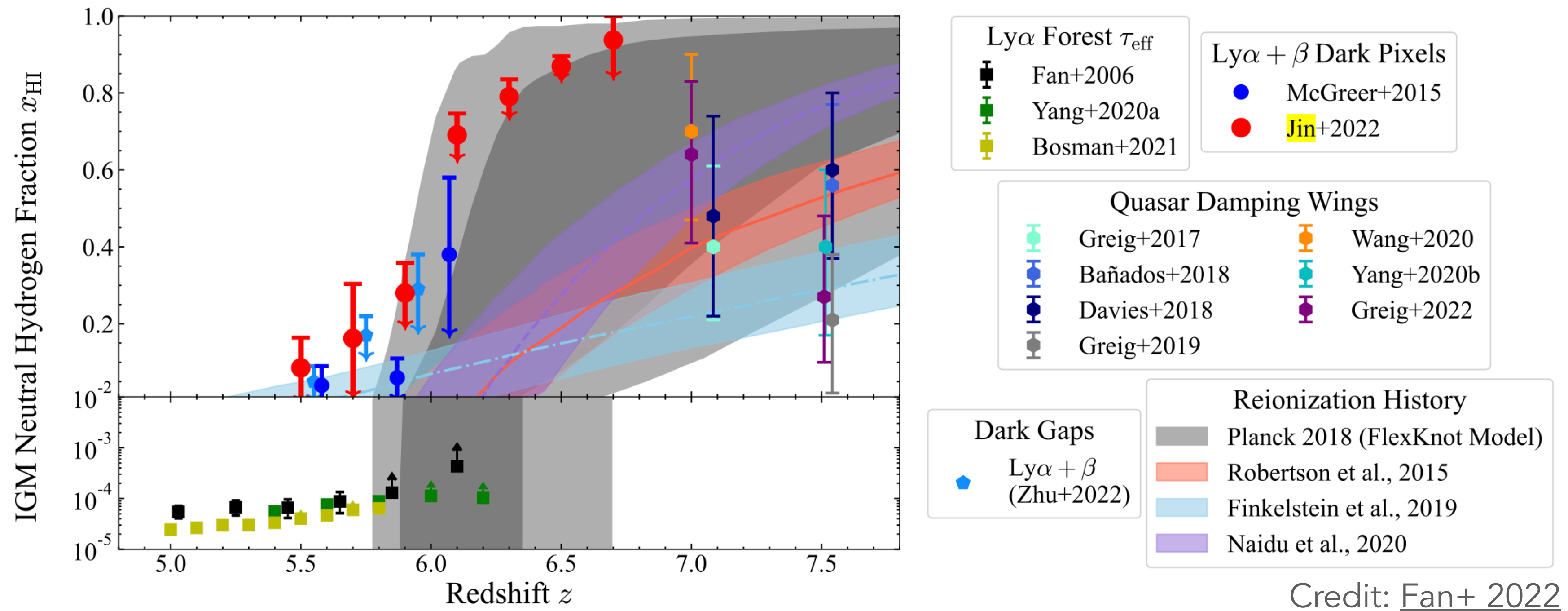
Quasars in a Reionizing Universe

Proximity Zones & IGM Damping Wings



Quasars in a Reionizing Universe

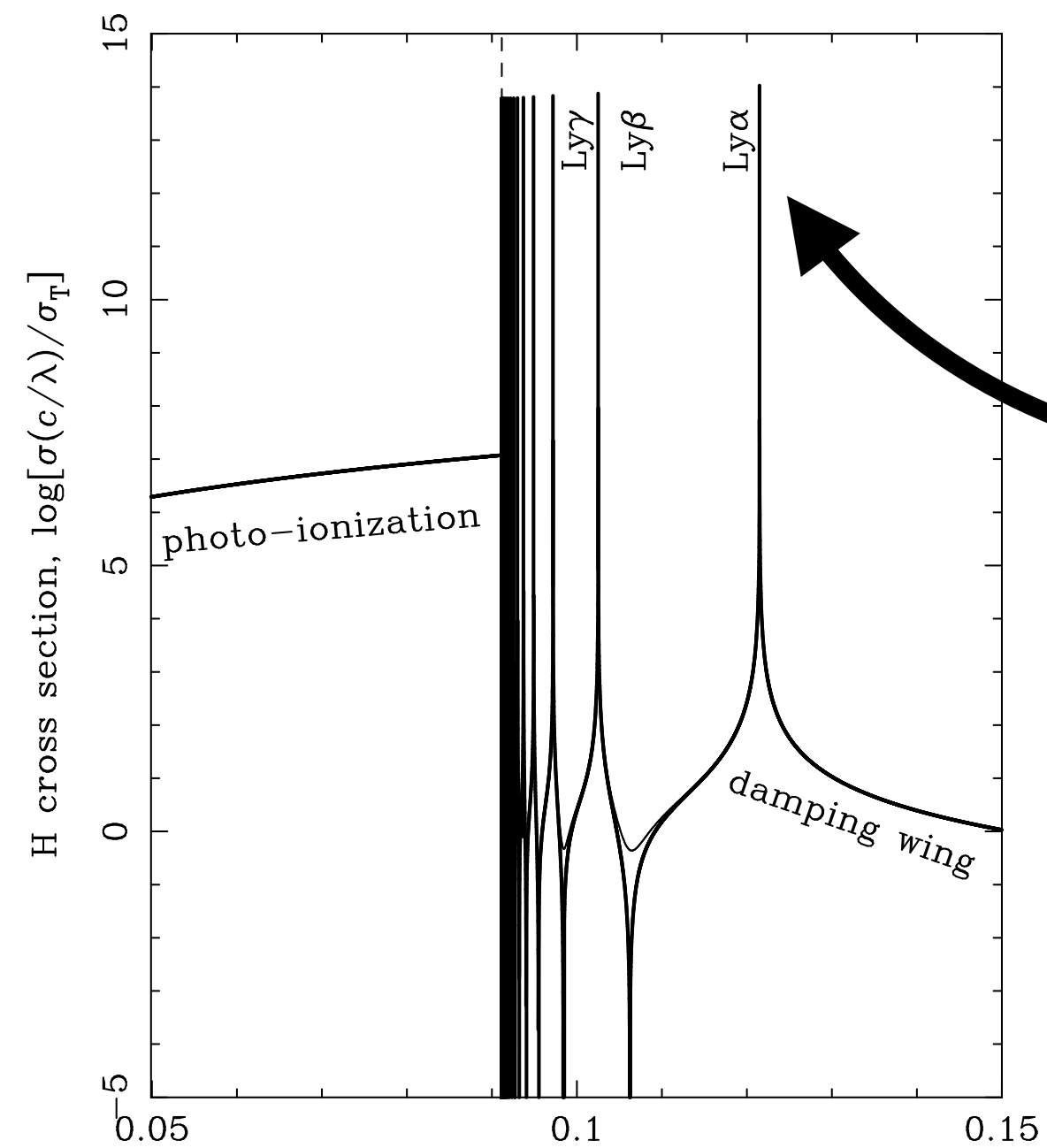
Proximity Zones & IGM Damping Wings



Quasars in a Reionizing Universe

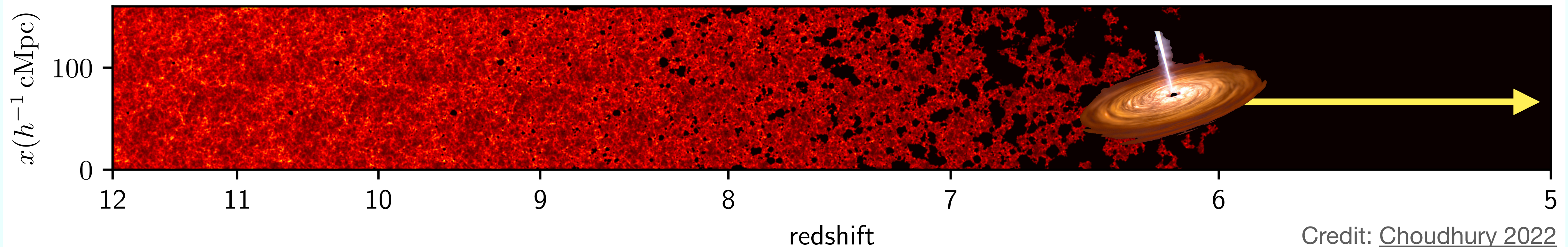
Proximity Zones & IGM Damping Wings

HI cross section



wavelength, λ (μm) Credit: [Mortlock 2016](#)

Ly α cross section so high that neutral fractions of $\langle x_{\text{HI}} \rangle \gtrsim 10^{-5}$ are enough to cause complete absorption in the Ly α forest (Gunn-Peterson trough)

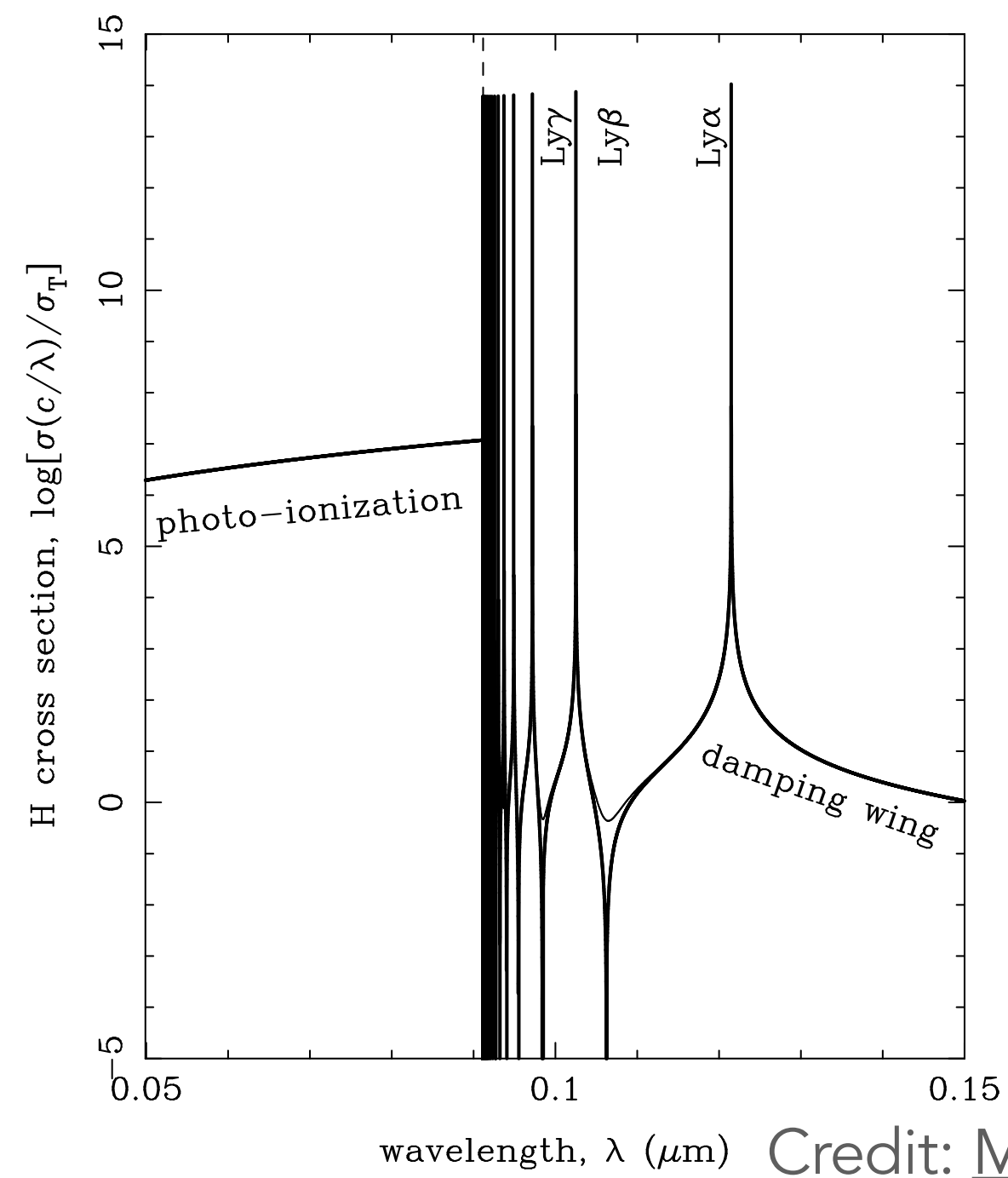


Credit: [Choudhury 2022](#)

Quasars in a Reionizing Universe

Proximity Zones & IGM Damping Wings

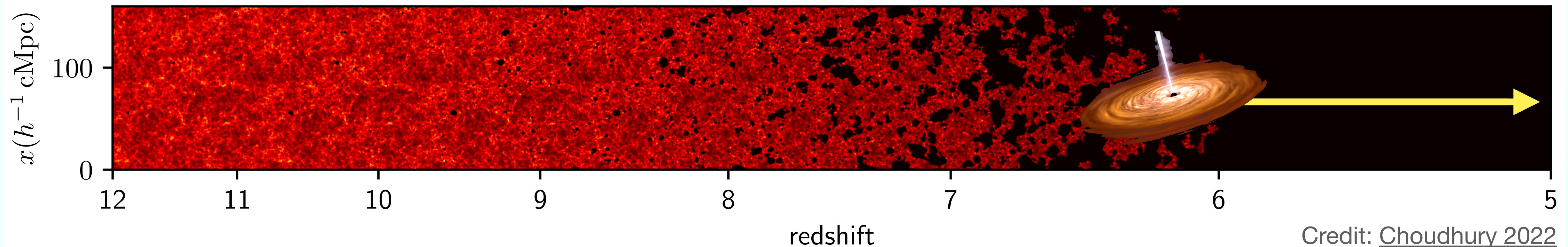
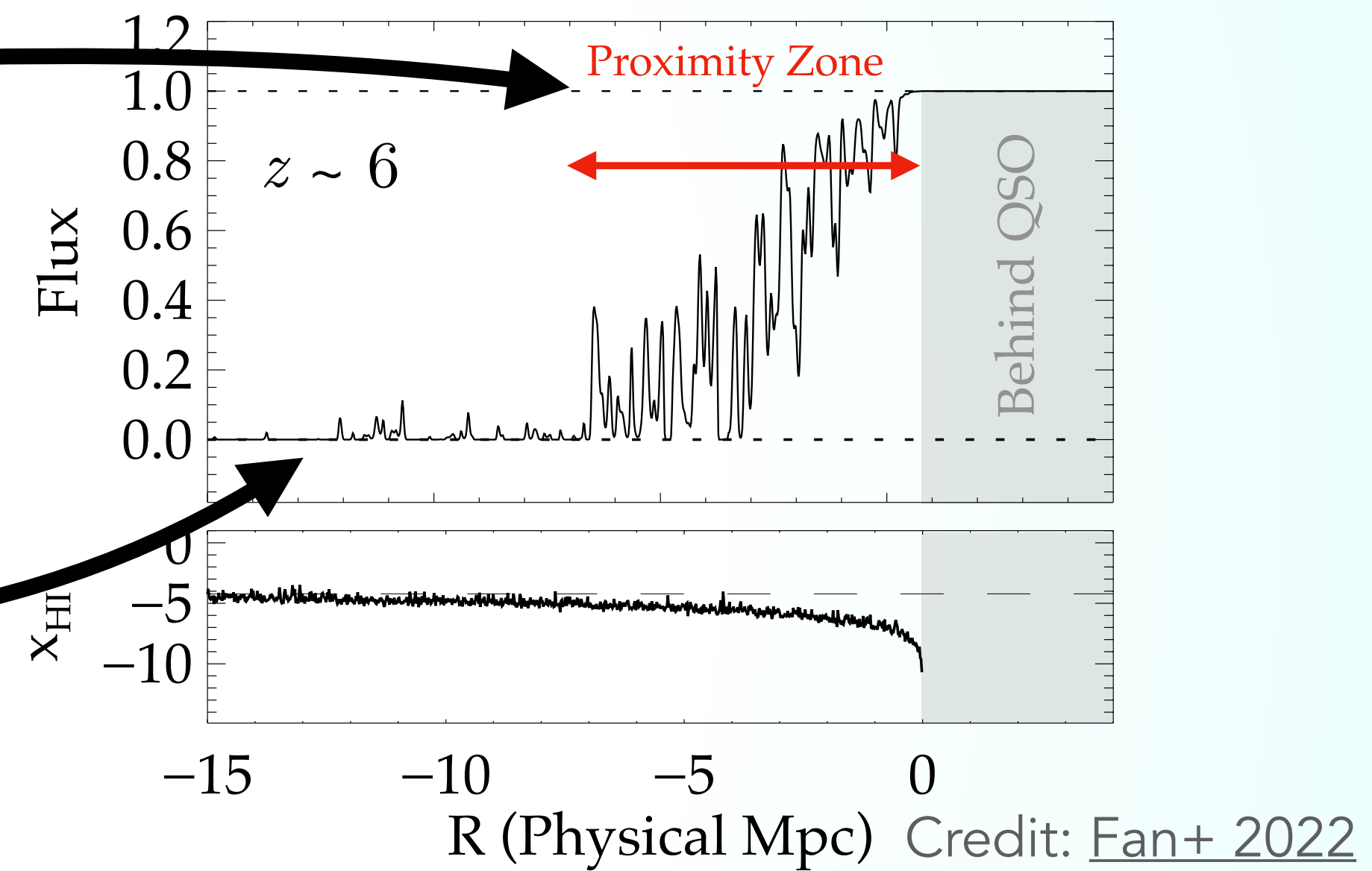
HI cross section



Proximity zone:

Non-zero transmission in the quasar's proximity due to its strong ionizing radiation

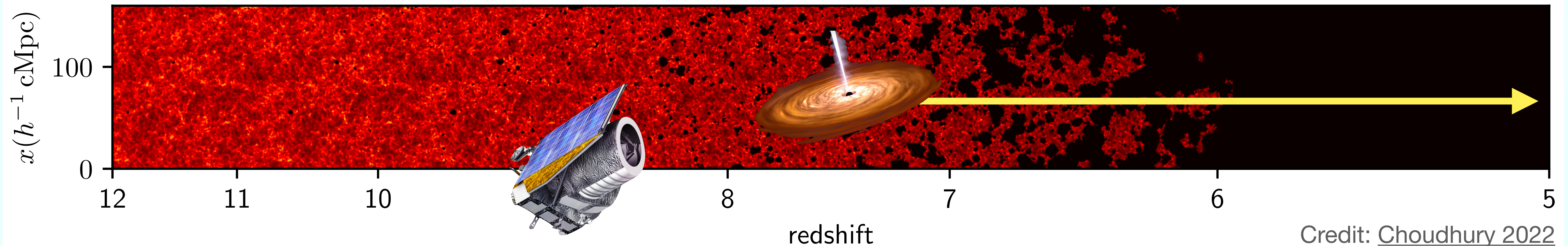
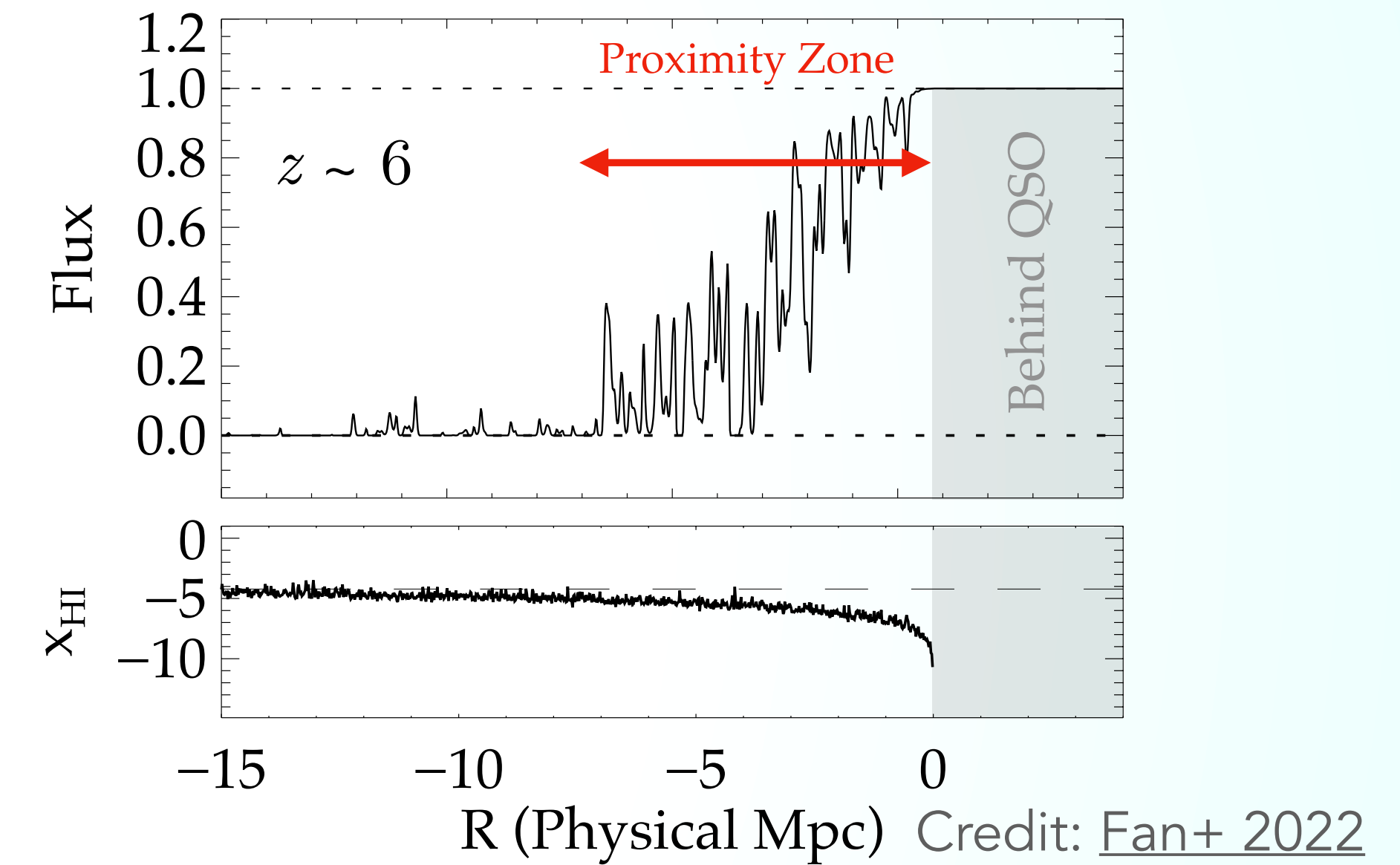
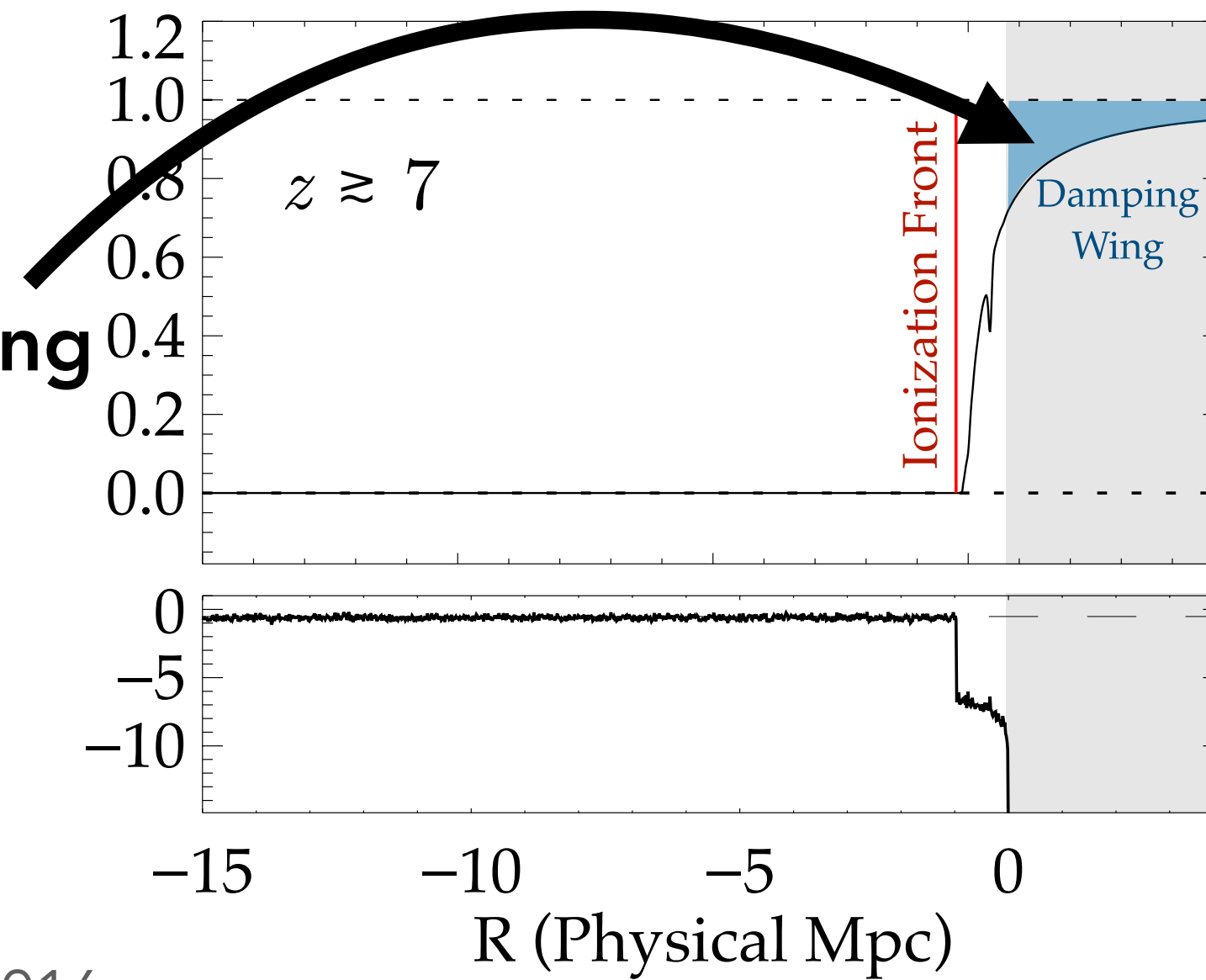
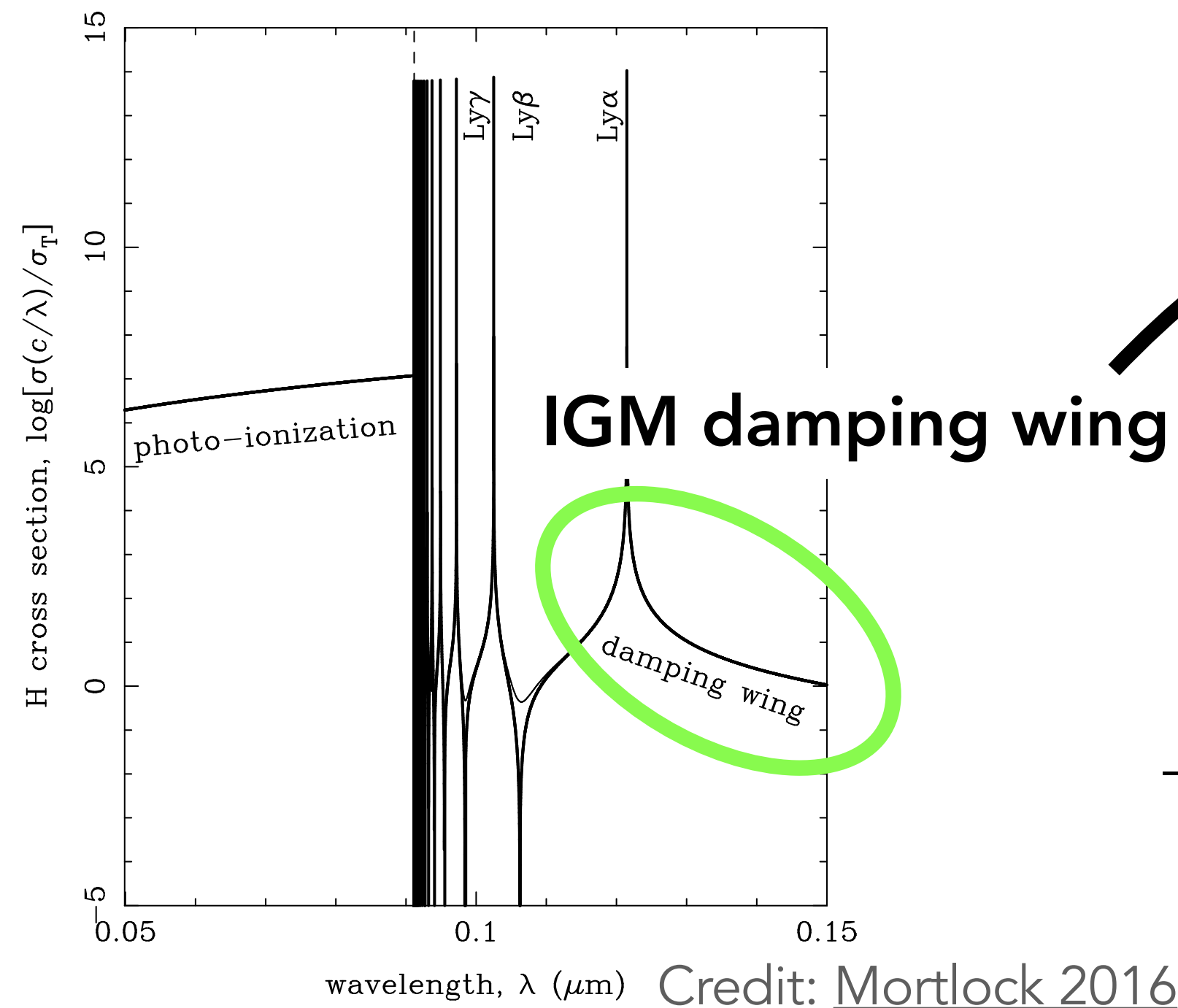
Gunn-Peterson trough



Quasars in a Reionizing Universe

Proximity Zones & IGM Damping Wings

HI cross section



Forward-Modelling Damping Wing Absorption

Constructing realistic skewers based on cosmological simulations

Nyx hydrodynamical simulations:

1200 density and temperature skewers around the most massive DM halos

21cmFast:

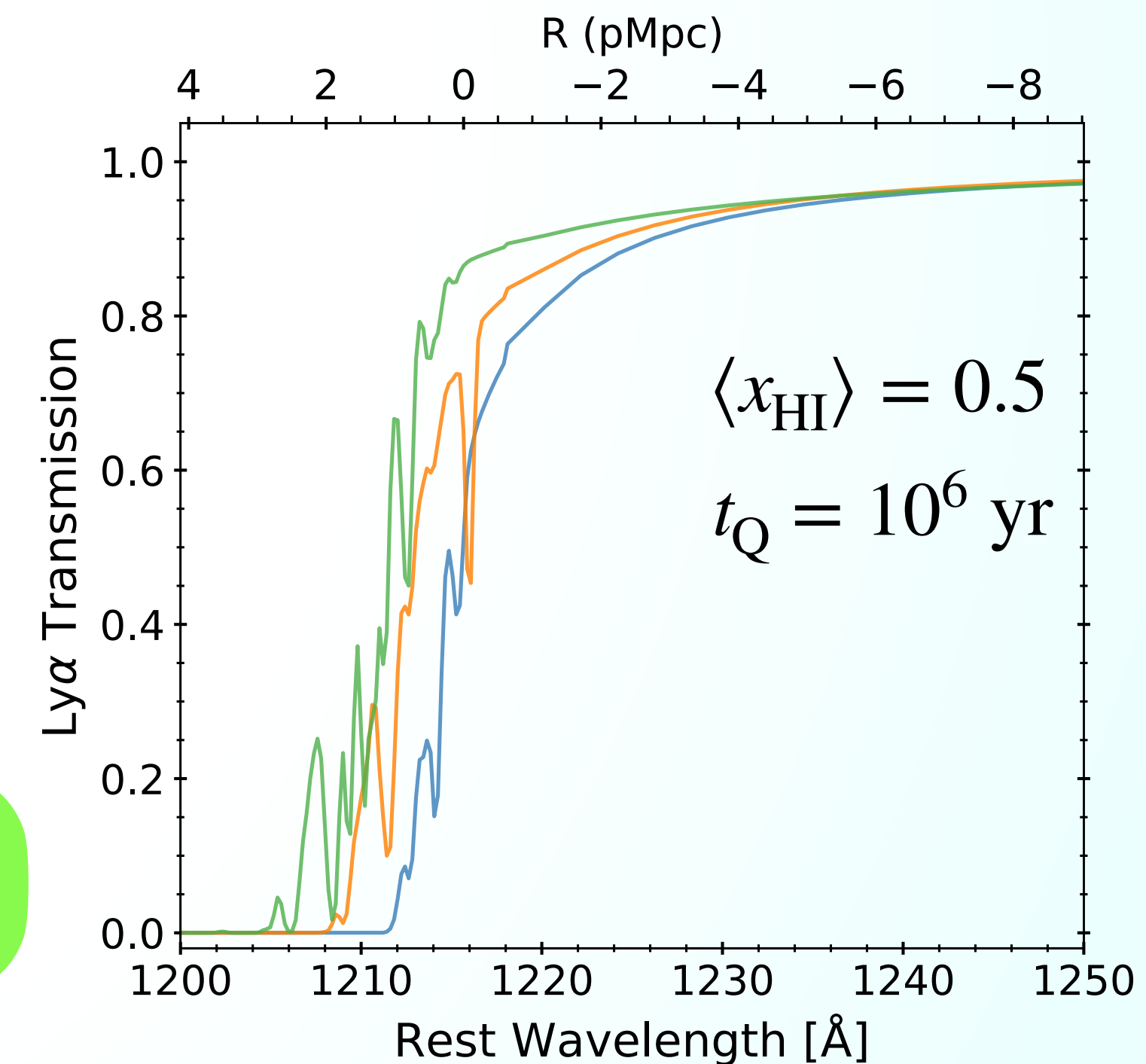
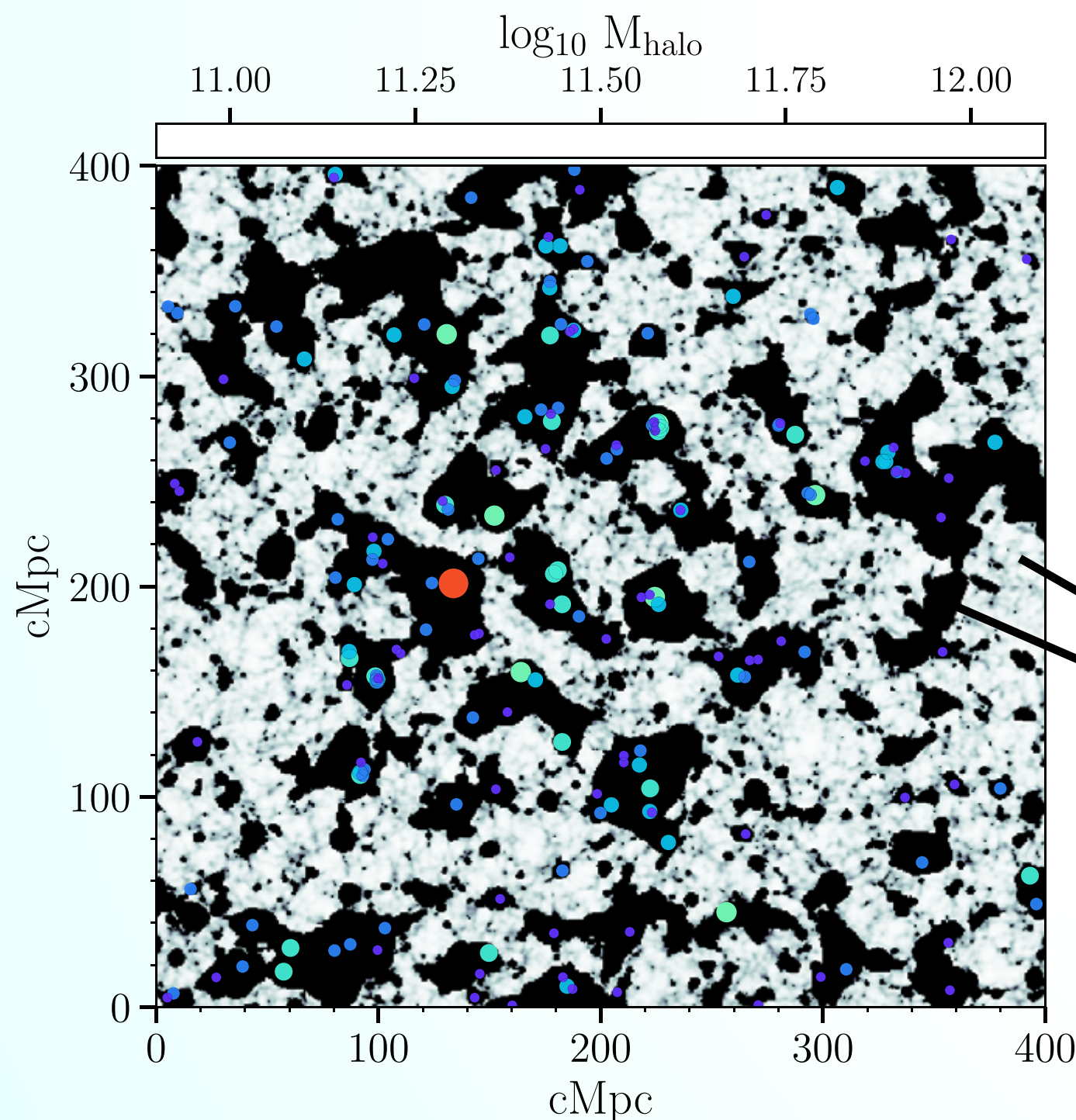
21 reionization topologies ($0 \leq \langle x_{\text{HI}} \rangle \leq 1$) with 10 000 x_{HI} skewers each

1D Radiative Transfer

51 quasar lifetimes between $10^3 \text{ yr} \leq t_{\text{Q}} \leq 10^8 \text{ yr}$

white: neutral
black: ionized

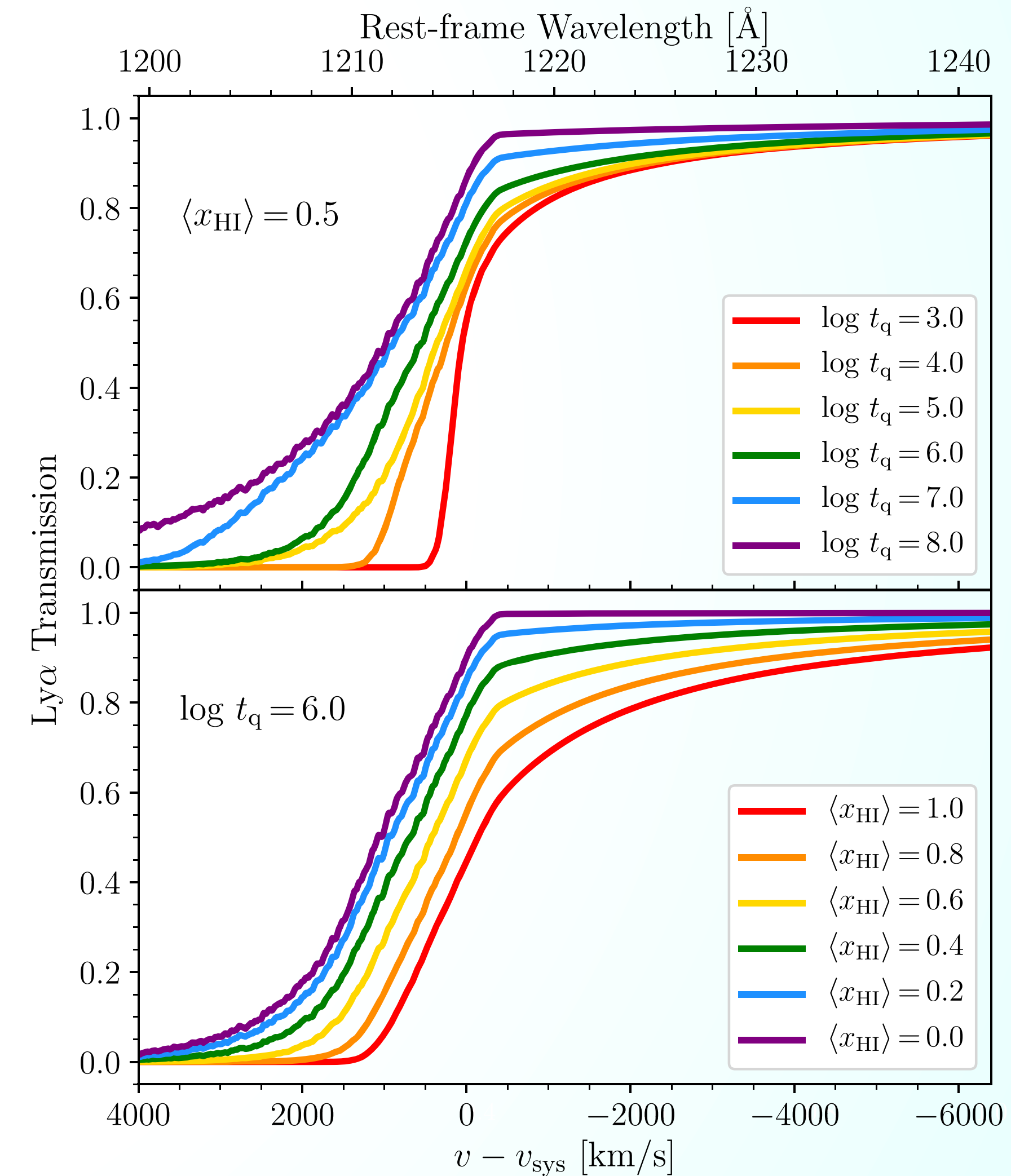
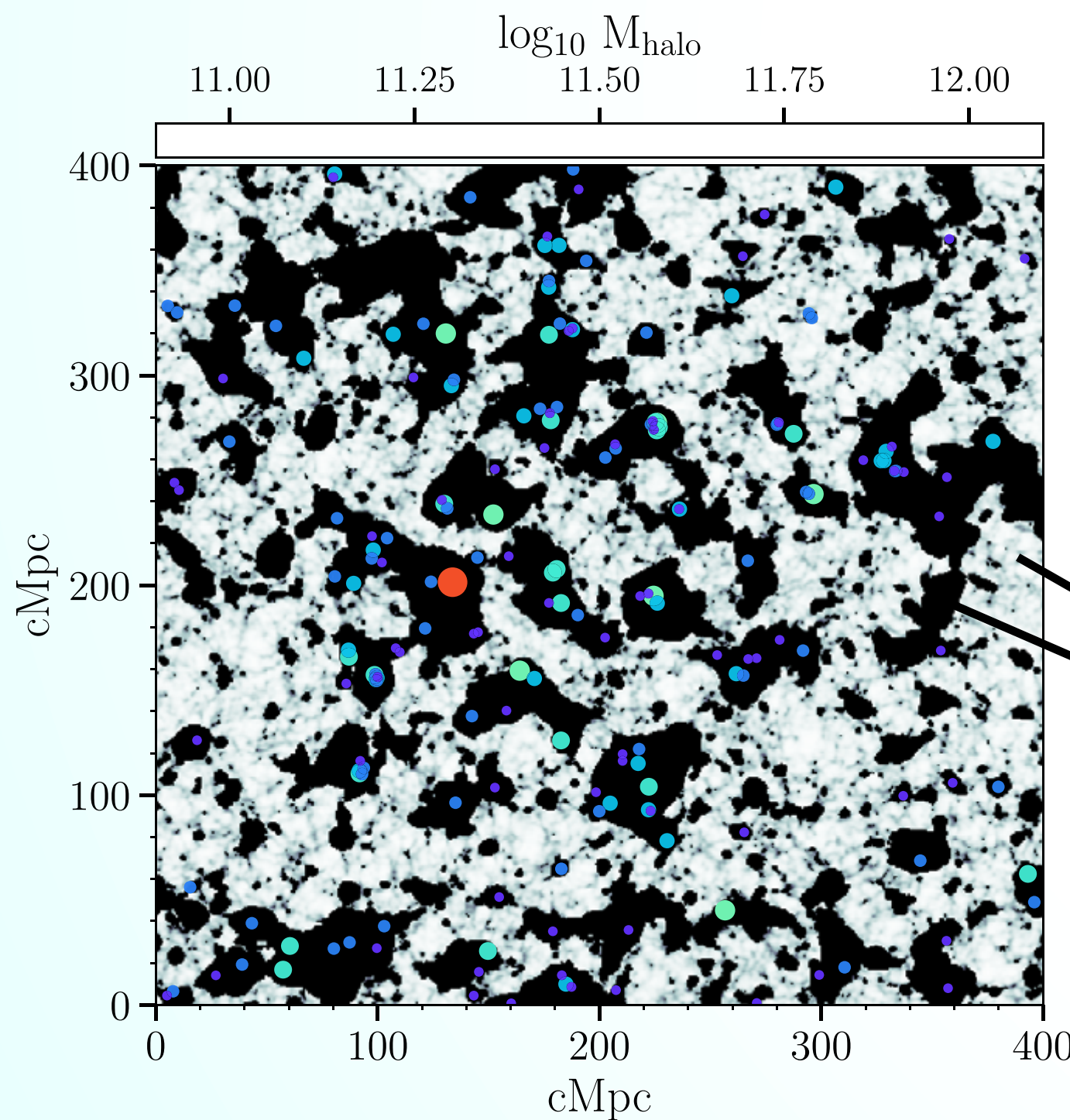
1200 x 21 x 51 grid of Ly- α transmission skewers



Forward-Modelling Damping Wing Absorption

Constructing realistic skewers based on cosmological simulations

Damping wing signature of high-redshift quasars allows inferring IGM neutral fraction $\langle x_{\text{HI}} \rangle$ and quasar lifetime t_{Q}



From an Observed Quasar Spectrum to $\langle x_{\text{HI}} \rangle$

Astrophysical Parameter Inference

DATA

Real or mock quasar spectrum with observational noise

MODEL

Quasar continuum model

Reconstruction error stochastic process

+

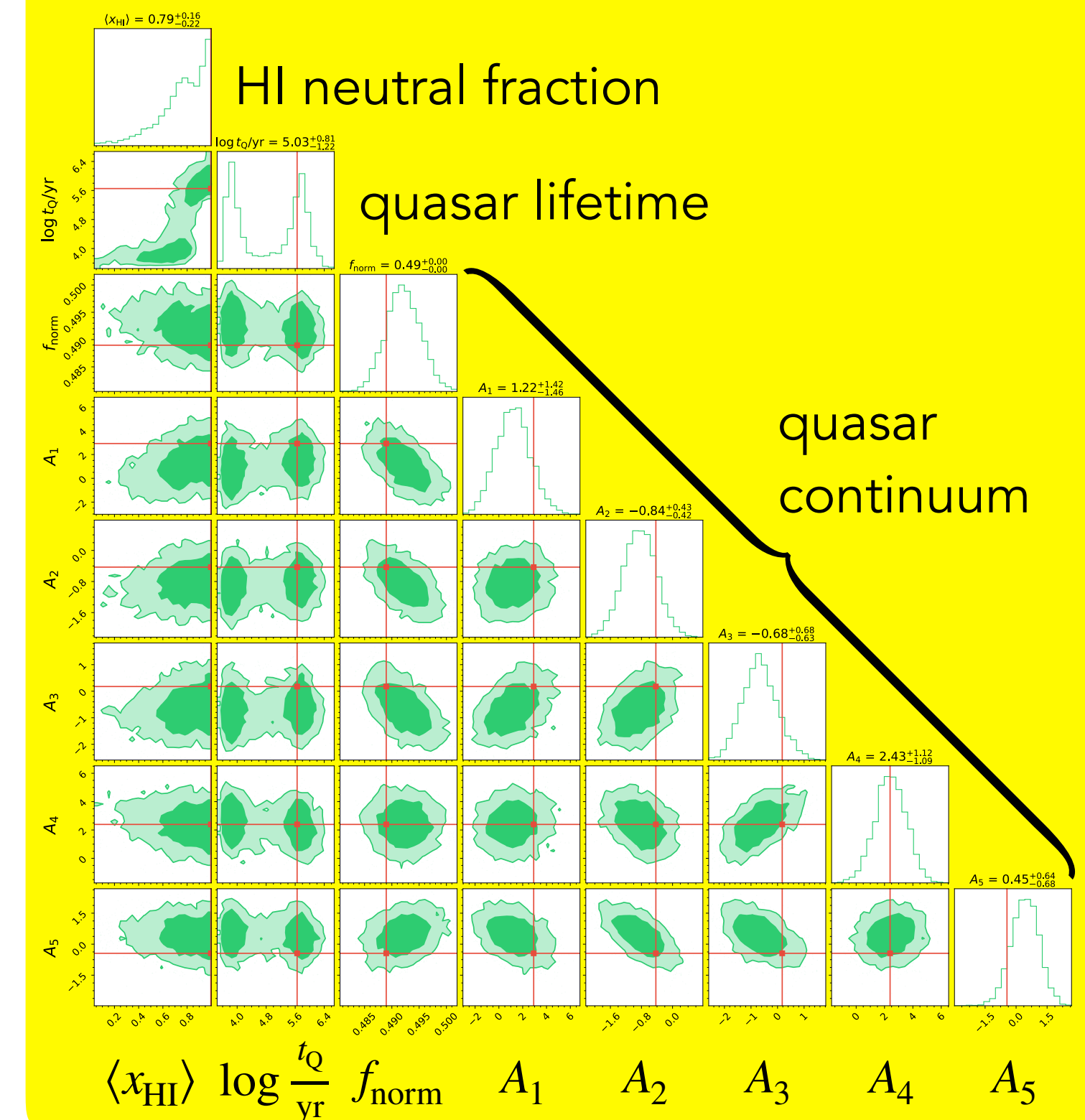
Ly- α transmission field stochastic process

BAYESIAN INFERENCE

with an analytical Gaussian likelihood approximation

- Likelihood operates on the **entire** spectrum (no red-blue split)
- Fast GPU-accelerated HMC implementation (runtimes \lesssim 1 hour)

POSTERIOR

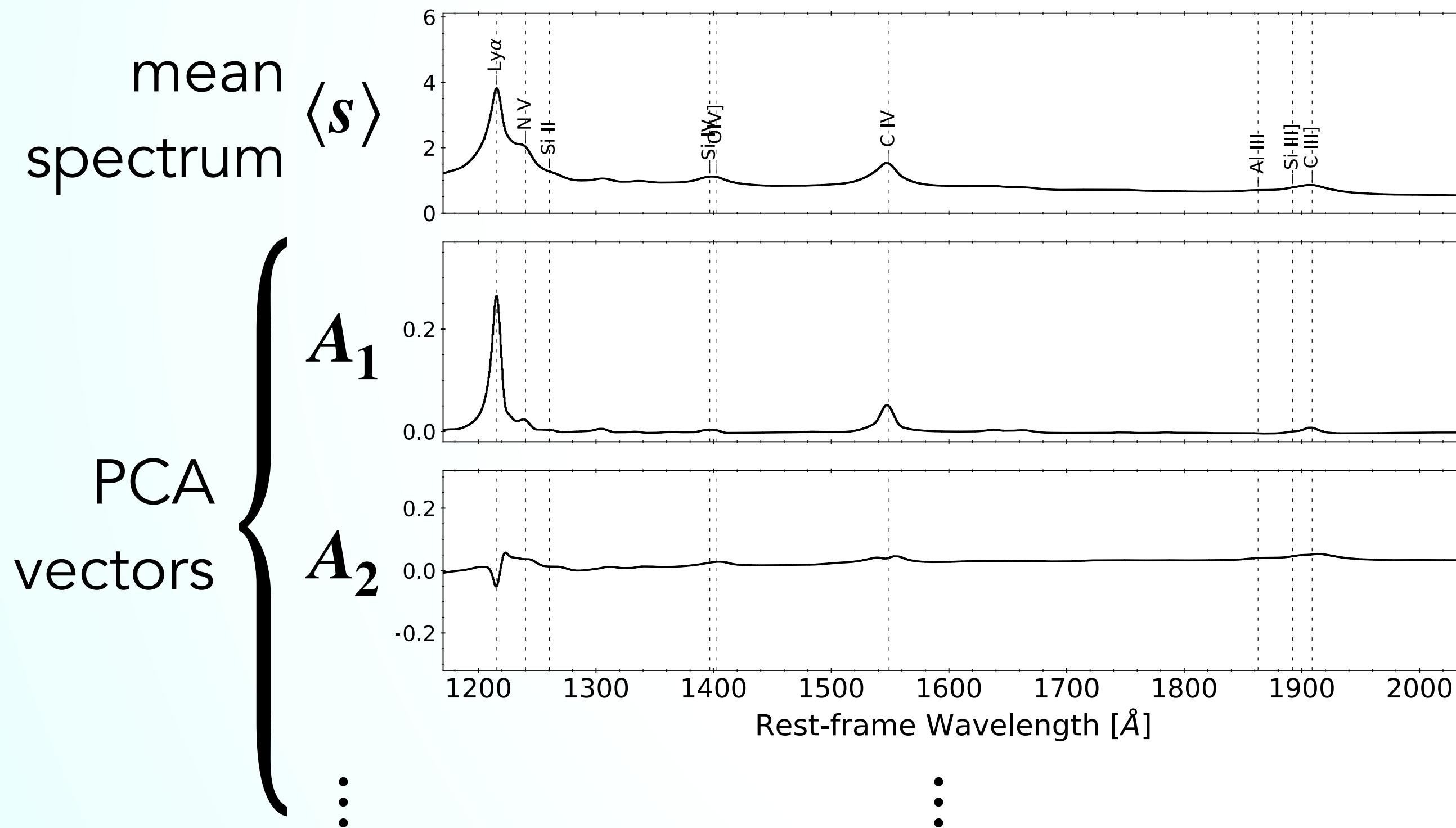


A PCA Model for the Quasar Continuum

Old-fashioned Dimensionality Reduction

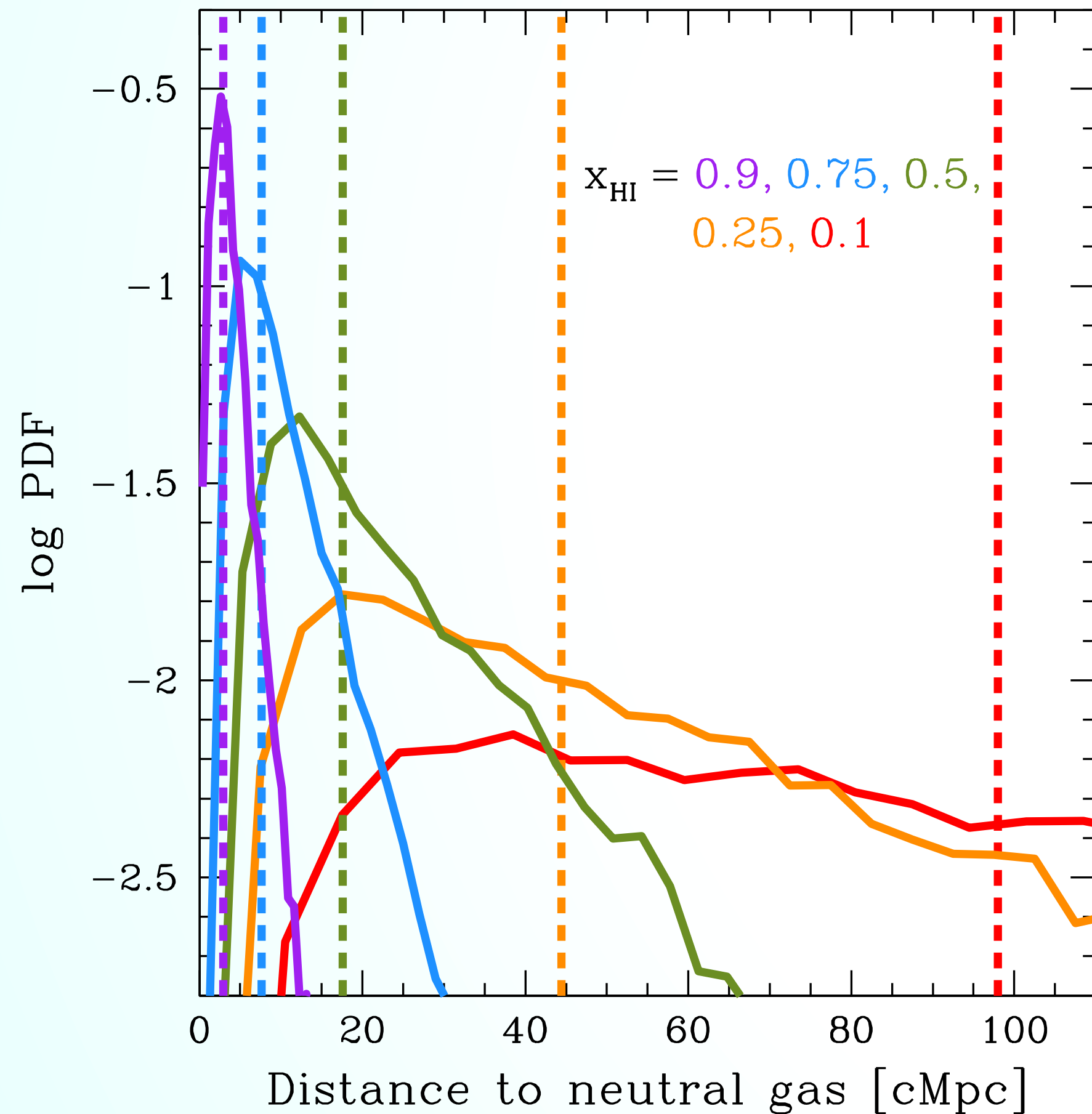
PCA decomposed spectrum $s_{\text{DR}}(\alpha) = \langle s \rangle + \alpha \cdot A$

- 15 559 SDSS-autofit continua ($2.149 < z < 4$, $R \sim 2000$, $S/N > 10$)
- 95% - 5% training-test split:
 - Training set of 14 781 continua to build PCA model
 - Test set of 778 continua to draw mock continua and estimate reconstruction error



Forward-Modelling Damping Wing Absorption

Eliminating the stochasticity of the bubble size distribution



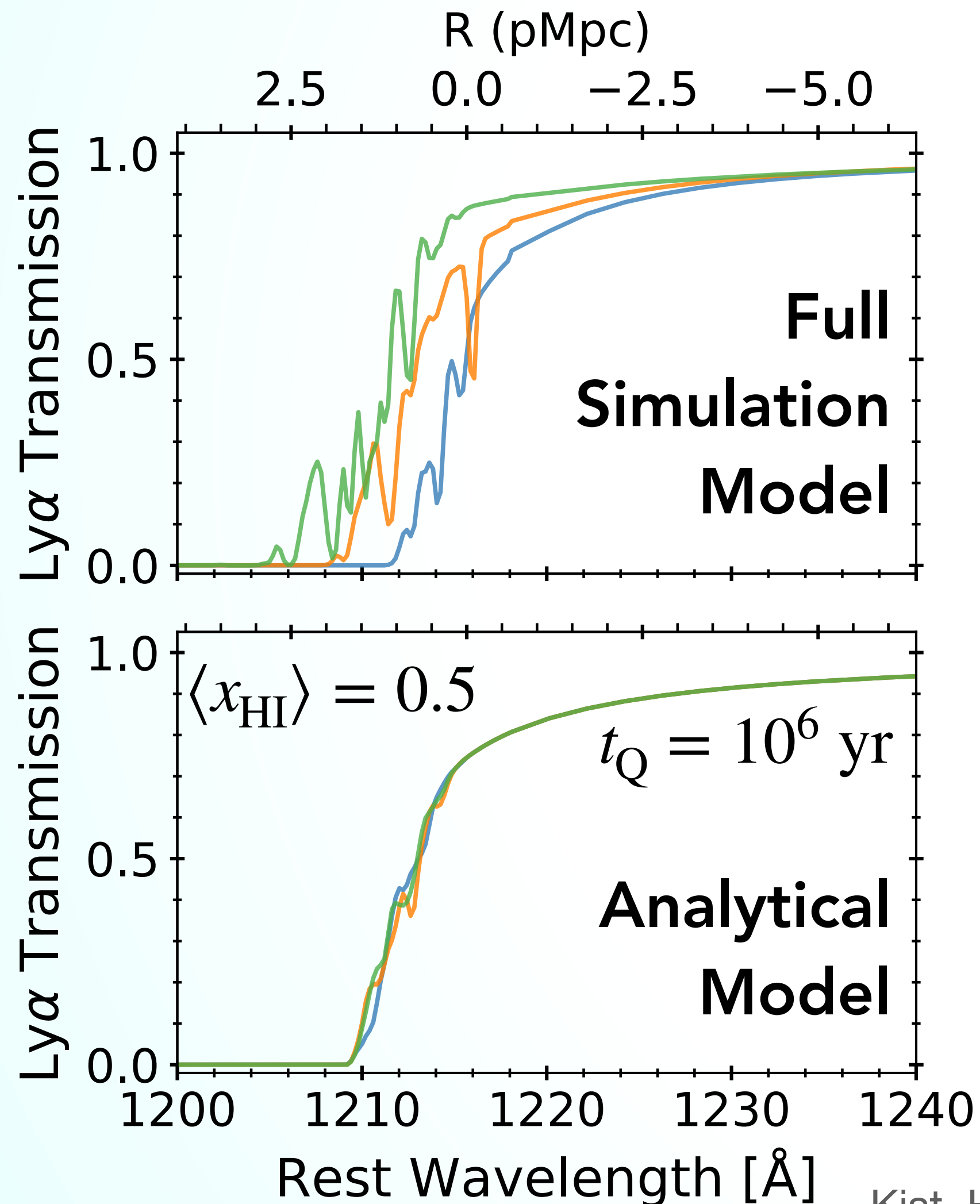
Credit: [Davies+ 2018](#)

- Ionised bubble sizes in simulation model depend stochastically on $\langle x_{\text{HI}} \rangle$
- For analysis purposes, eliminate this stochasticity by building a simple analytic model (c.f. [Mortlock 2016](#)):
 - Radius of the ionisation front:

$$R_{\text{ion}} \simeq 12.0 \text{ cMpc} \times (t_{\text{Q}}/\text{Myr})^{1/3} \langle x_{\text{HI}} \rangle^{-1/3}$$
 - Damping wing optical depth determined deterministically in terms of R_{ion} (c.f. [Miralda-Escudé 1998](#))

Forward-Modelling Damping Wing Absorption

Eliminating the stochasticity of the bubble size distribution

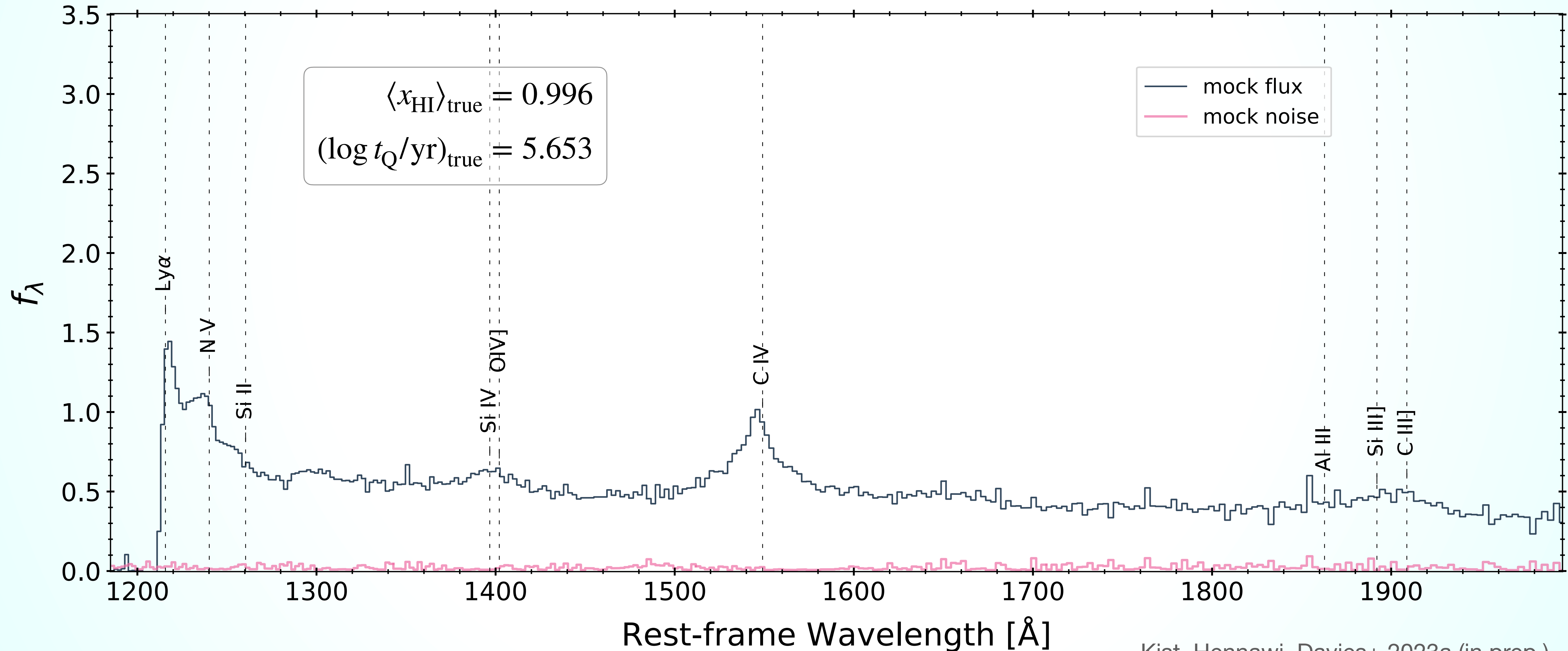


- Ionised bubble sizes in simulation model depend stochastically on $\langle x_{\text{HI}} \rangle$
- For analysis purposes, eliminate this stochasticity by building a simple analytic model (c.f. [Mortlock 2016](#)):
- Radius of the ionisation front:

$$R_{\text{ion}} \simeq 12.0 \text{ cMpc} \times (t_Q/\text{Myr})^{1/3} \langle x_{\text{HI}} \rangle^{-1/3}$$
- Damping wing optical depth determined deterministically in terms of R_{ion} (c.f. [Miralda-Escudé 1998](#))

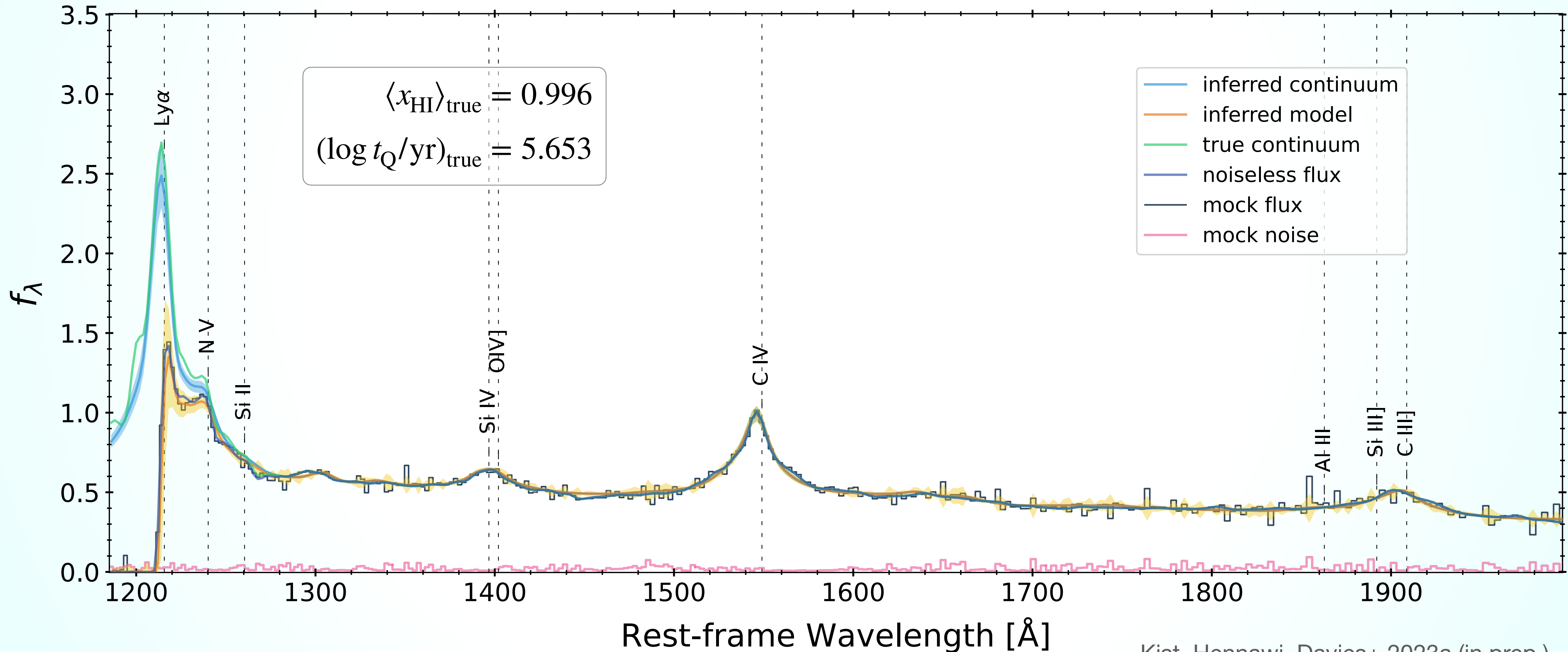
From an Observed Quasar Spectrum to $\langle x_{\text{HI}} \rangle$

A Quasar in a Neutral Environment



From an Observed Quasar Spectrum to $\langle x_{\text{HI}} \rangle$

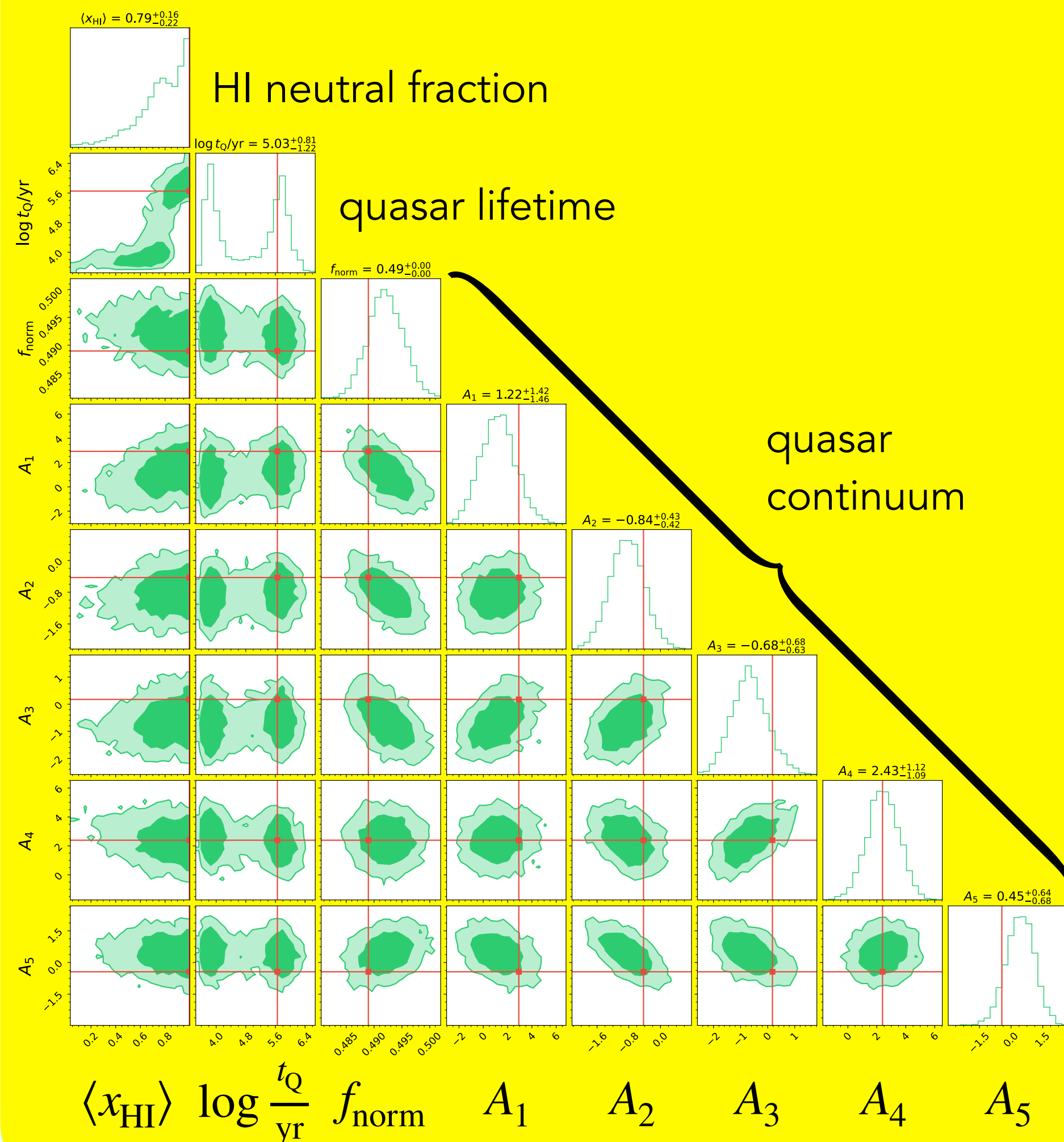
A Quasar in a Neutral Environment



From an Observed Quasar Spectrum to $\langle x_{\text{HI}} \rangle$

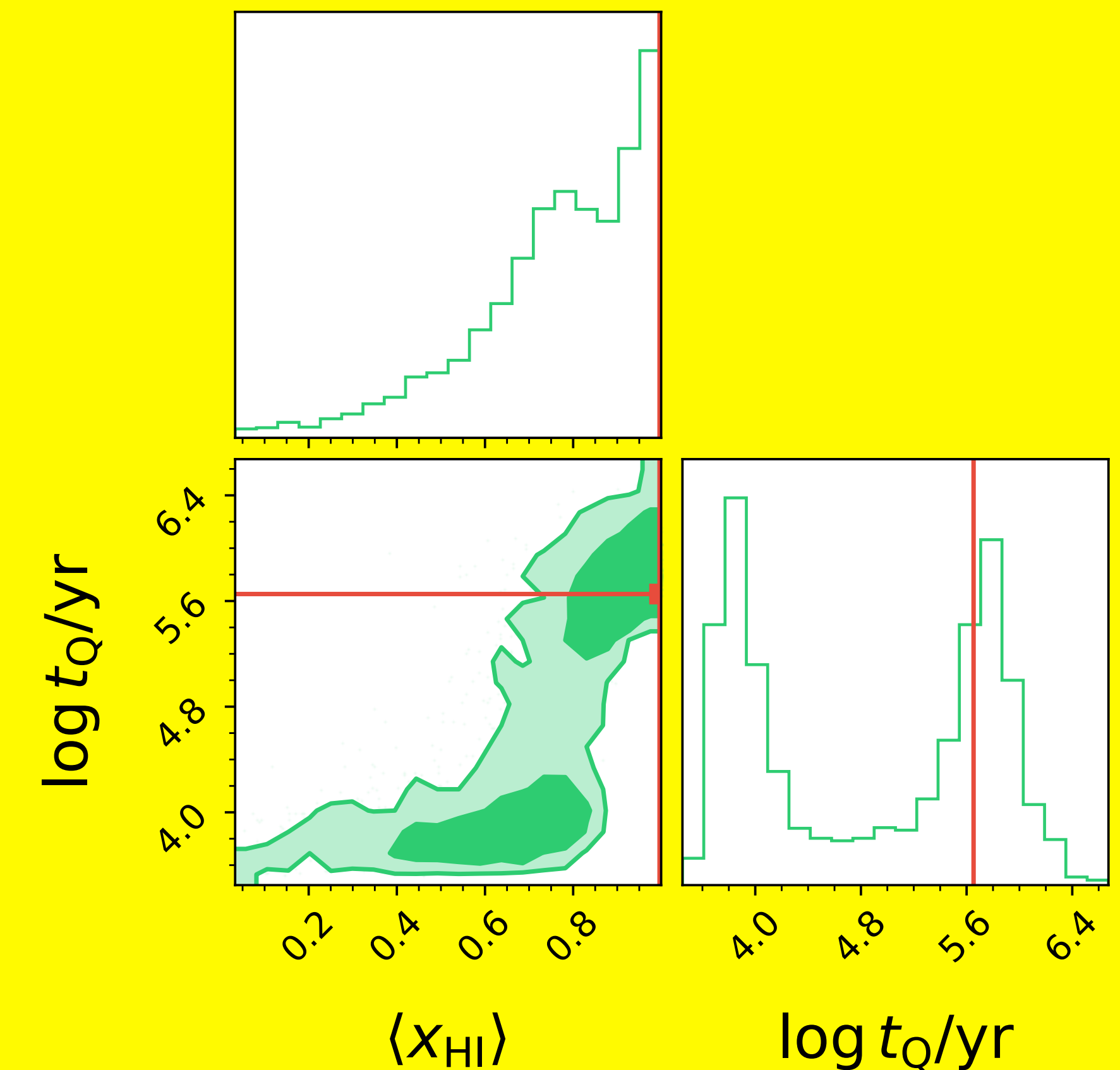
Posterior Distribution

Full 2+6-dimensional posterior distribution



Marginalizing over
6 continuum nuisance
parameters

Marginal $(\langle x_{\text{HI}} \rangle, t_Q)$ -posterior distribution



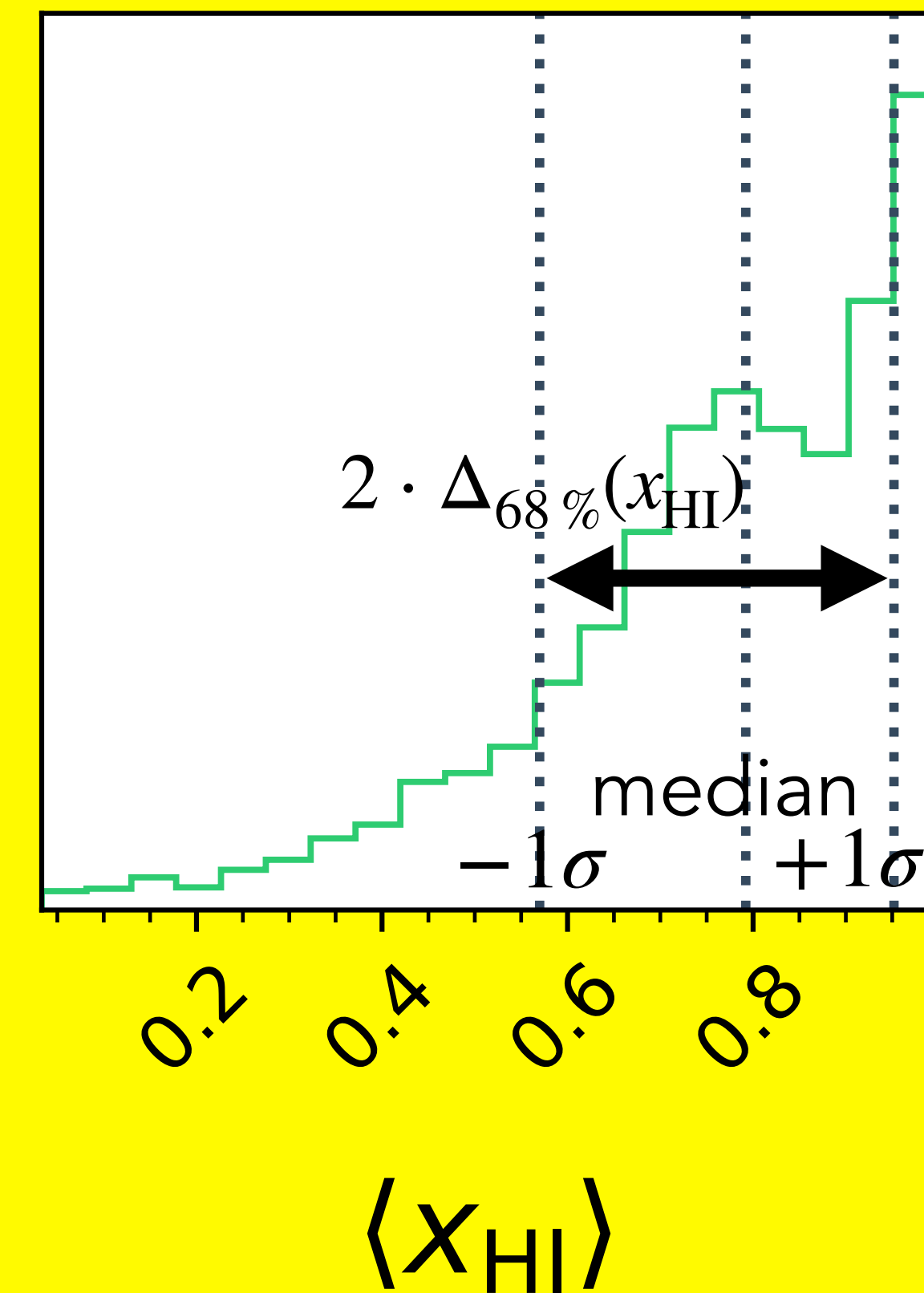
From an Observed Quasar Spectrum to $\langle x_{\text{HI}} \rangle$

Posterior Distribution

How does inference precision vary across parameter space?

What are the dominant contributions to the error budget?

Marginal $\langle x_{\text{HI}} \rangle$ -posterior distribution

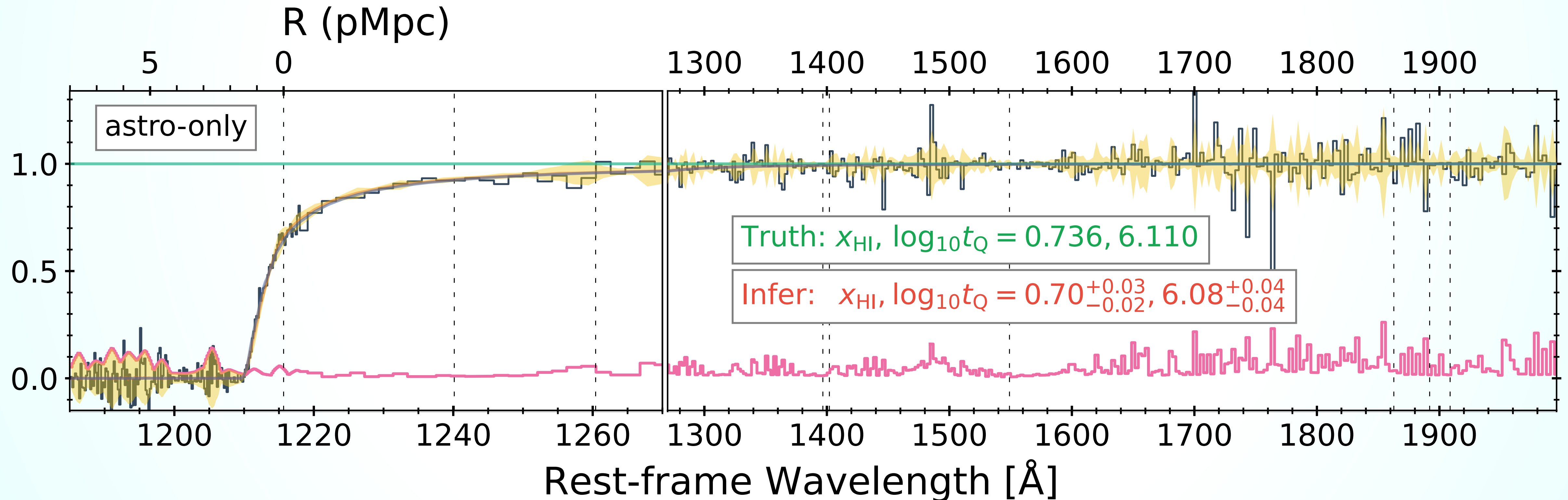


The PCA Continuum Model

Impact on Inference Precision

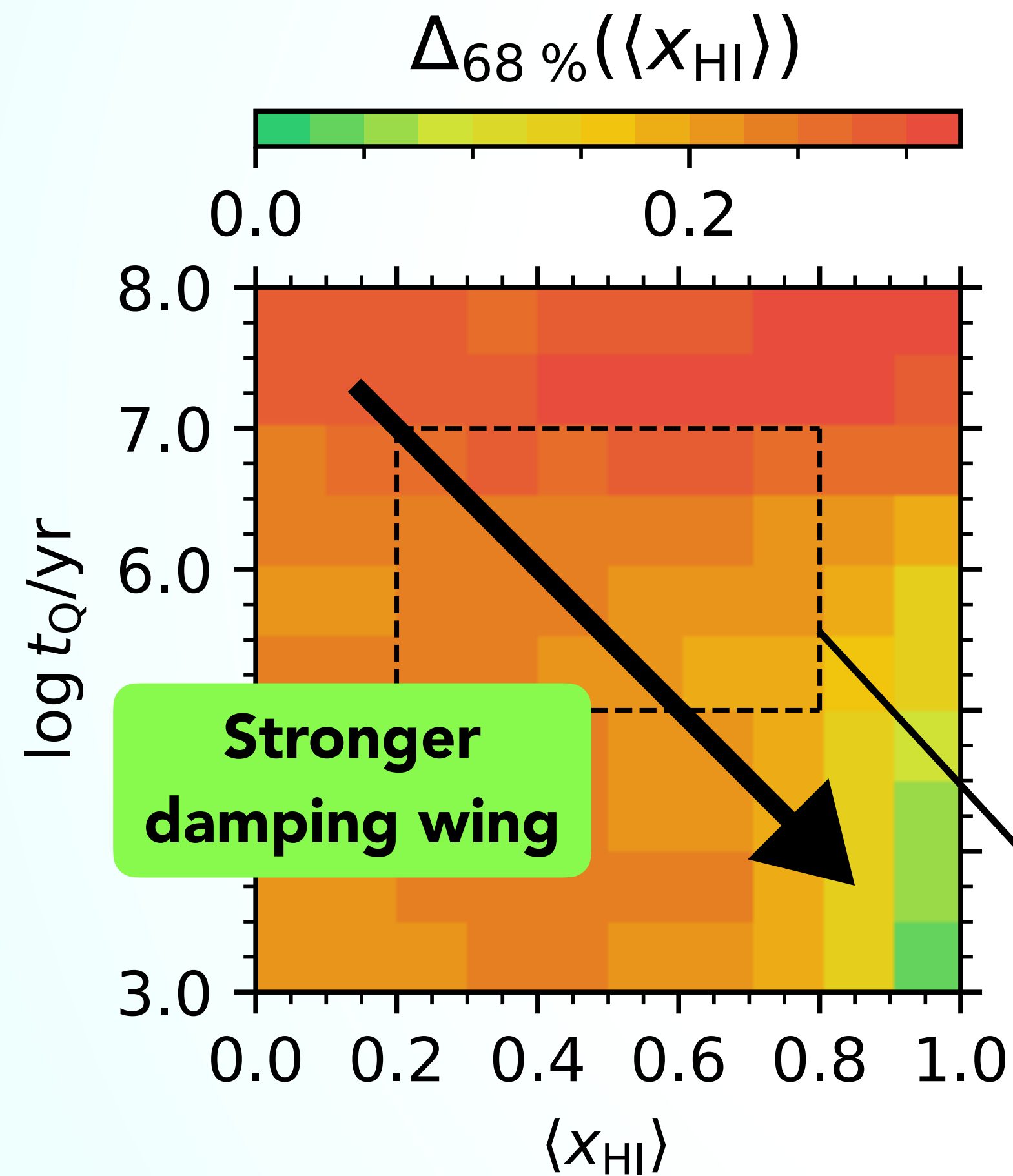
Continuum-normalized spectrum:

→ optimal bound on inferring $\langle x_{\text{HI}} \rangle$ and t_{Q} without nuisance parameters



Quantifying $\langle x_{\text{HI}} \rangle$ Inference Precision

Variation across Model Components and Parameter Space

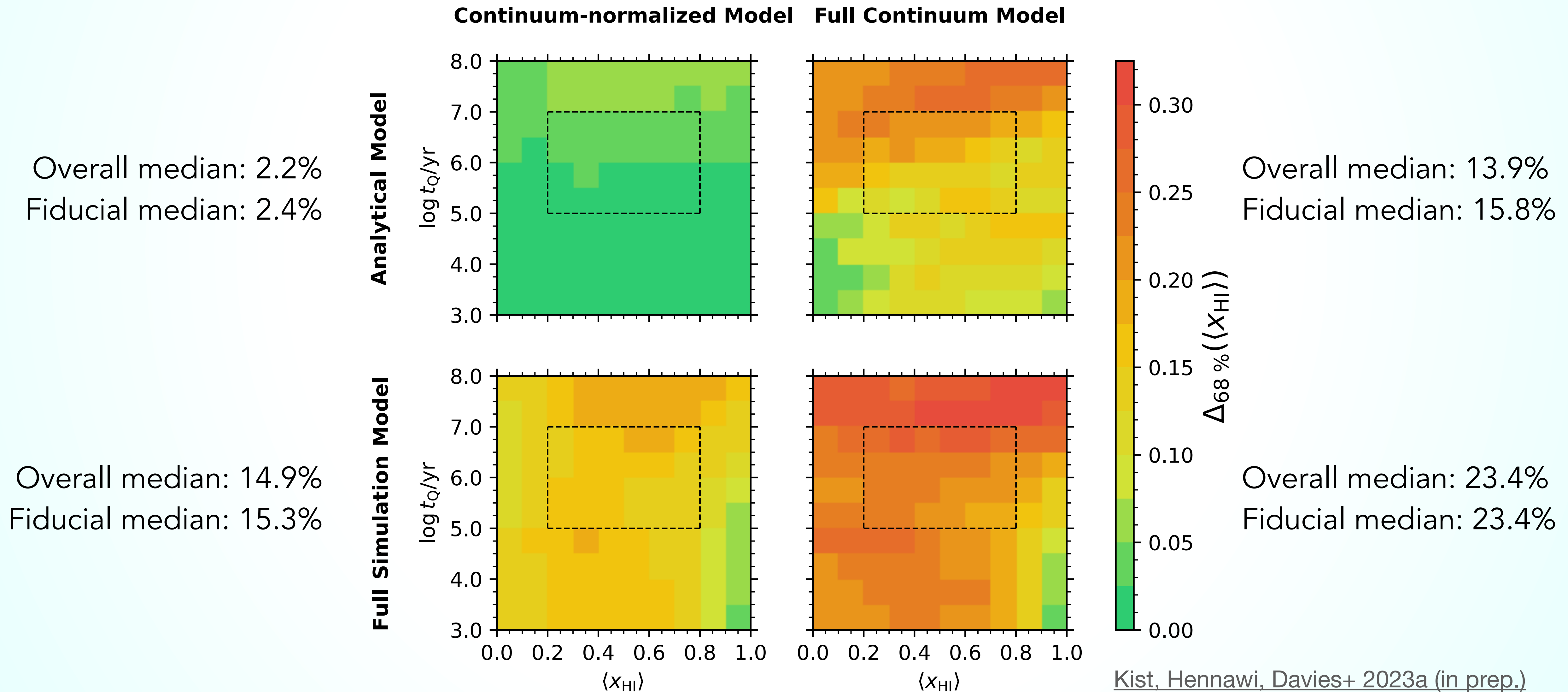


- Precision varies significantly across parameter space (between 2.6% and 39.3%)
- Median precision: 23.4%
- Stronger damping wing imprint (higher $\langle x_{\text{HI}} \rangle$, lower t_Q) improves precision

"Fiducial" region of parameter space

Quantifying $\langle x_{\text{HI}} \rangle$ Inference Precision

Variation across Model Components and Parameter Space

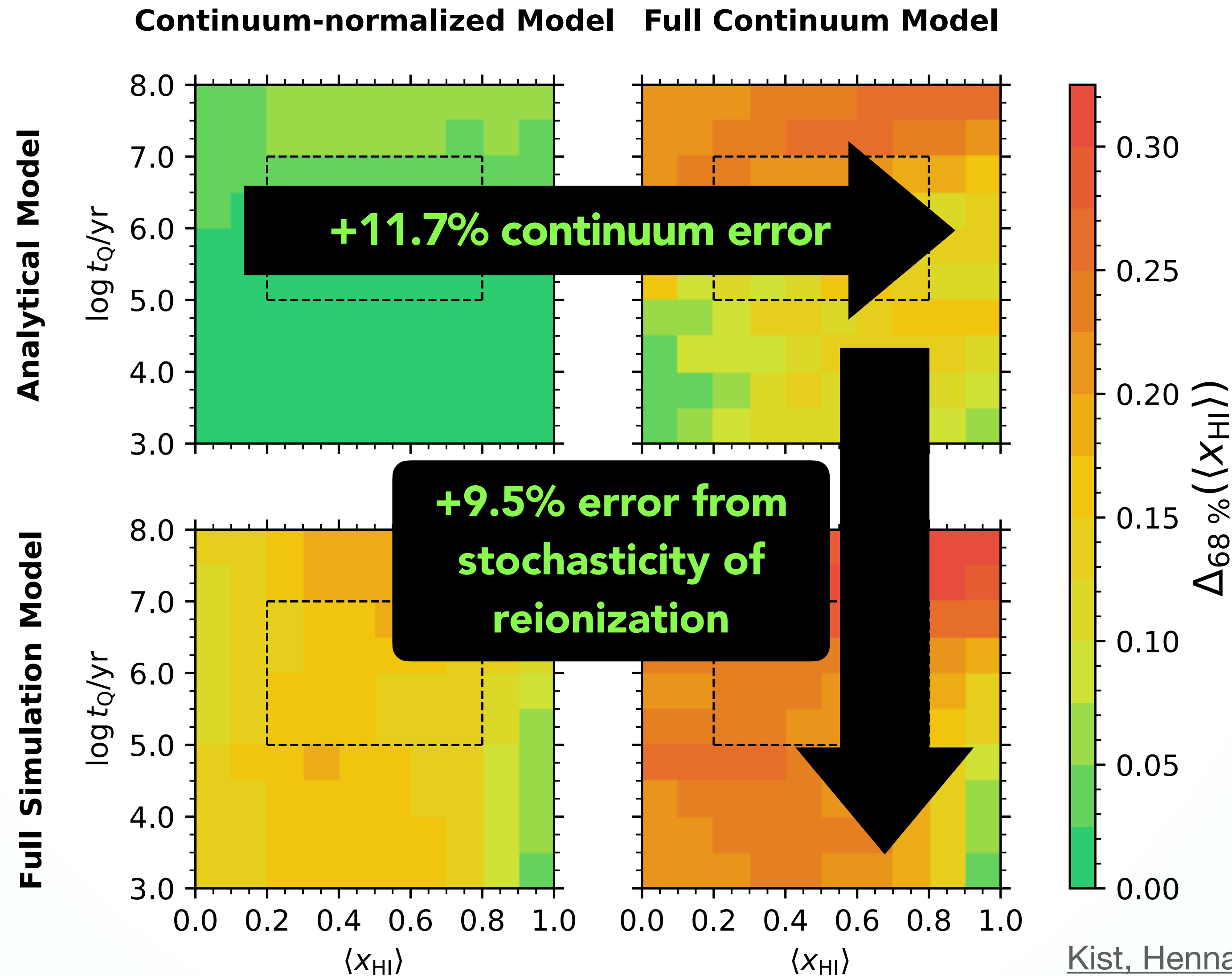


Quantifying $\langle x_{\text{HI}} \rangle$ Inference Precision

Variation across Model Components and Parameter Space

Overall median: 2.2%
Fiducial median: 2.4%

Overall median: 14.9%
Fiducial median: 15.3%

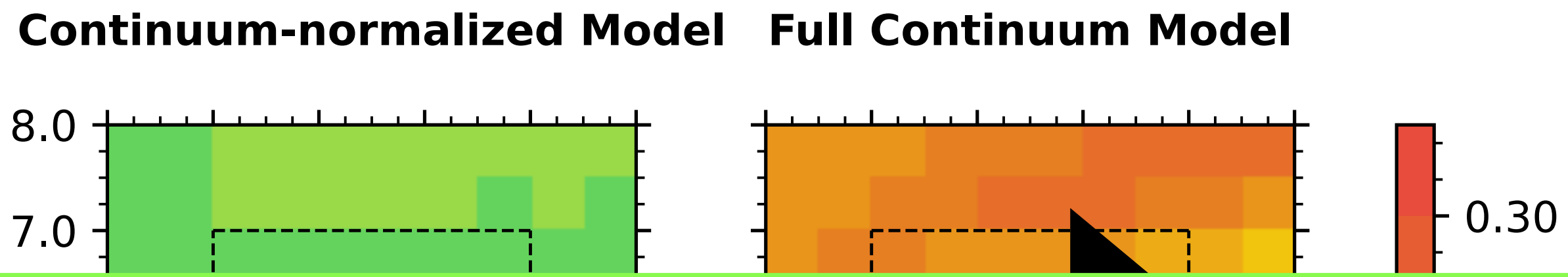


Overall median: 13.9%
Fiducial median: 15.8%

23.4% total
1 σ -uncertainty

Quantifying $\langle x_{\text{HI}} \rangle$ Inference Precision

Variation across Model Components and Parameter Space

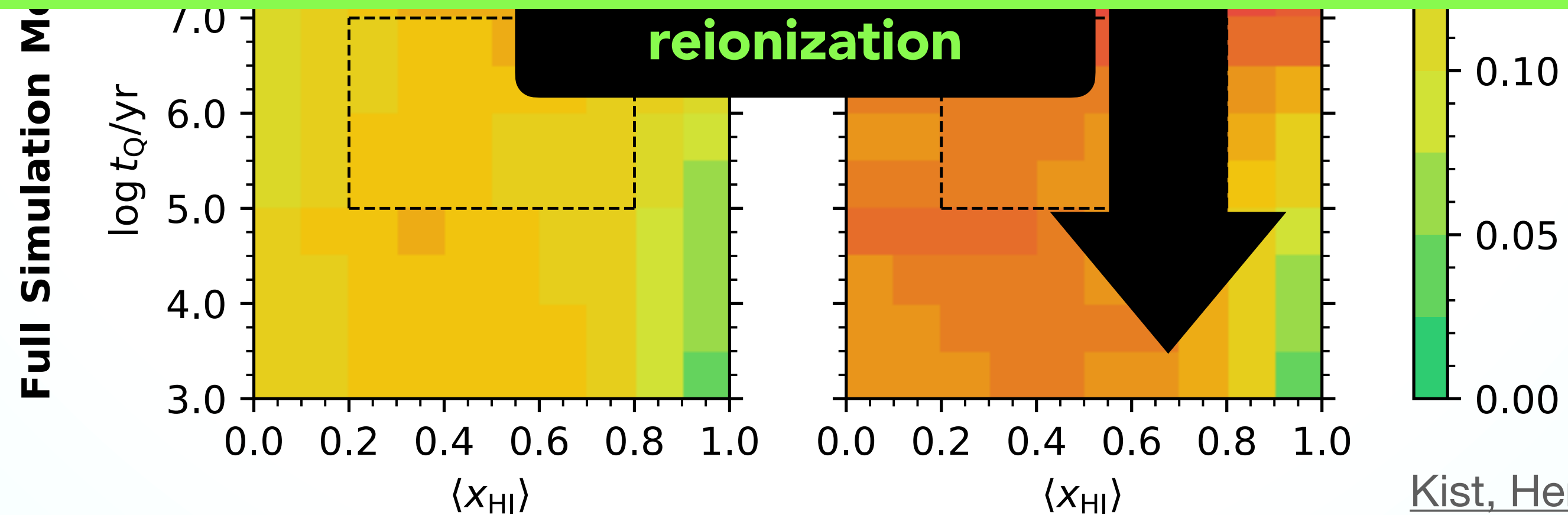


Overall
Fiducial

13.9%
15.8%

How tightly can we constrain the reionization history with data from upcoming surveys?

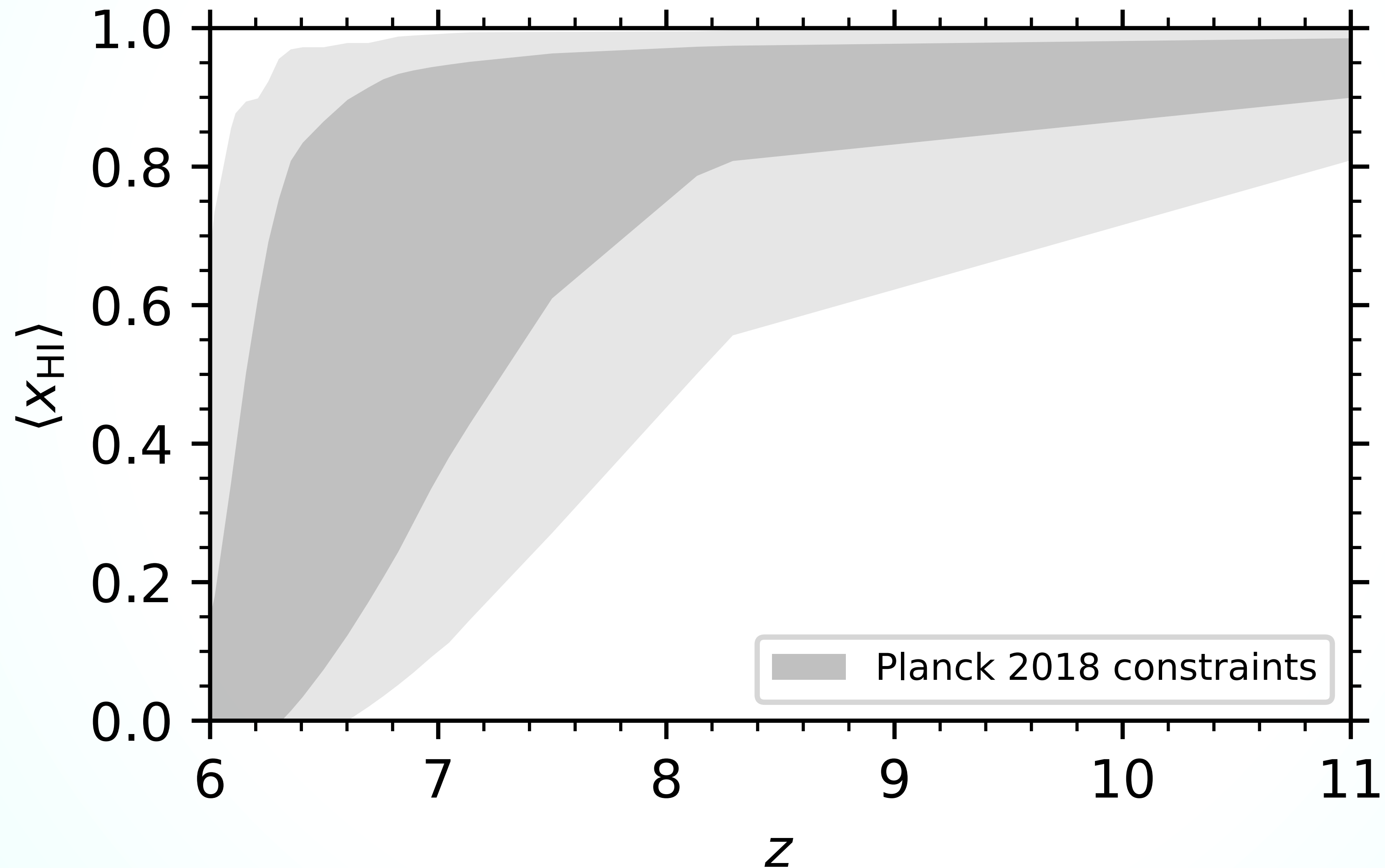
Overall median: 14.9%
Fiducial median: 15.3%



**23.4% total
 1σ -uncertainty**

Constraining Reionization History

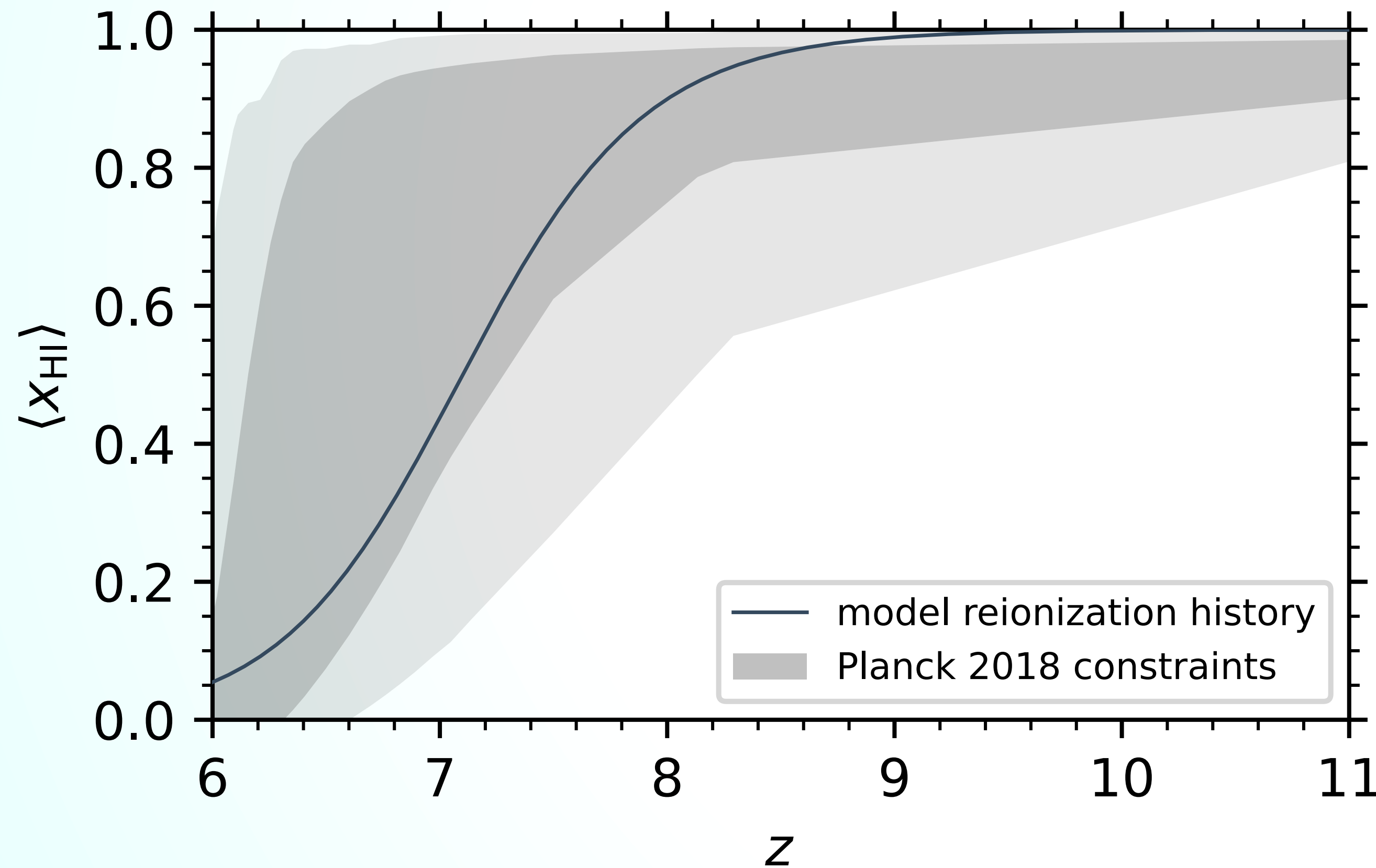
Current CMB constraints



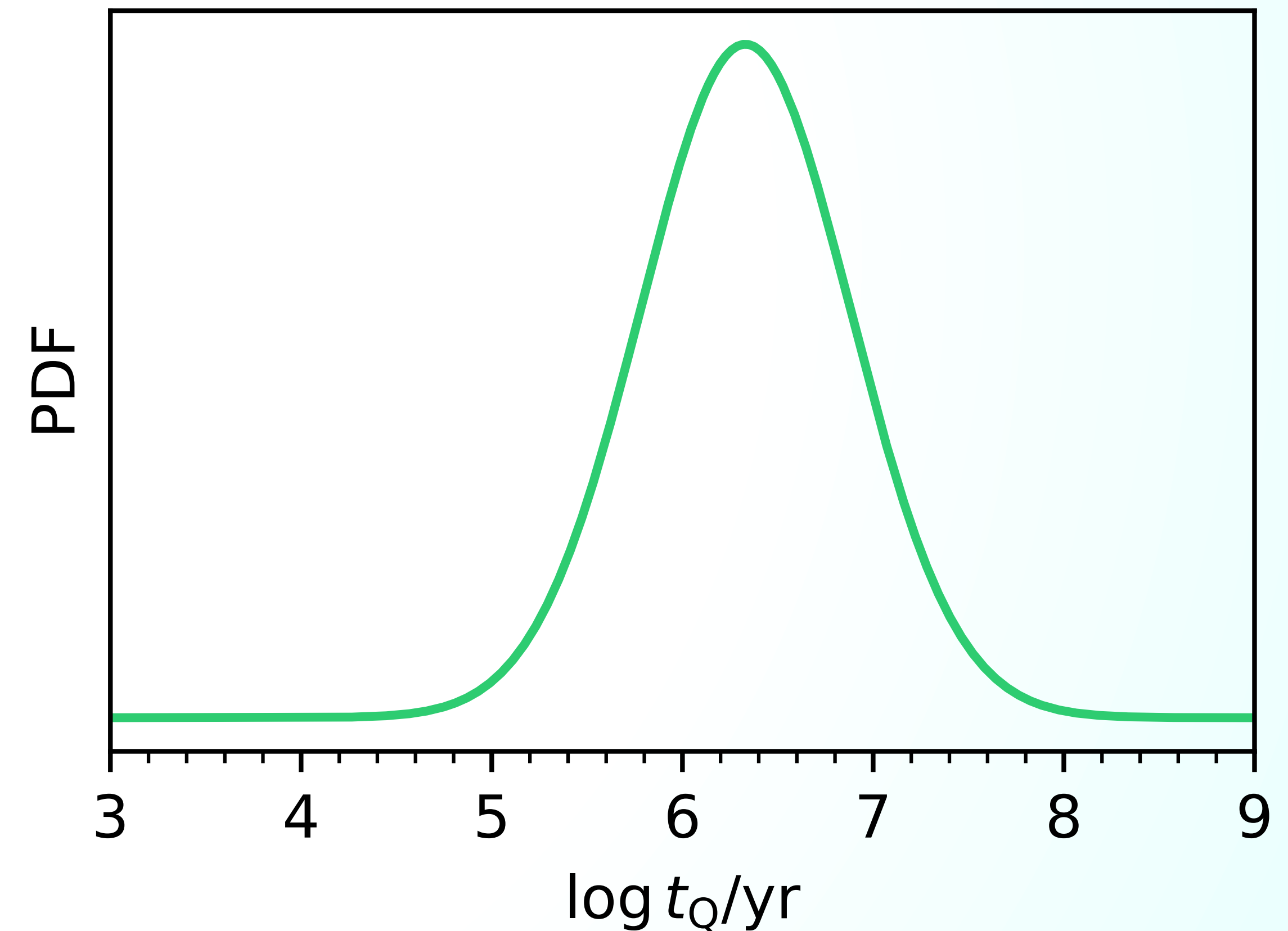
Constraining Reionization History

A forecast of upcoming EUCLID constraints

Toy model for $\langle x_{\text{HI}} \rangle(z)$

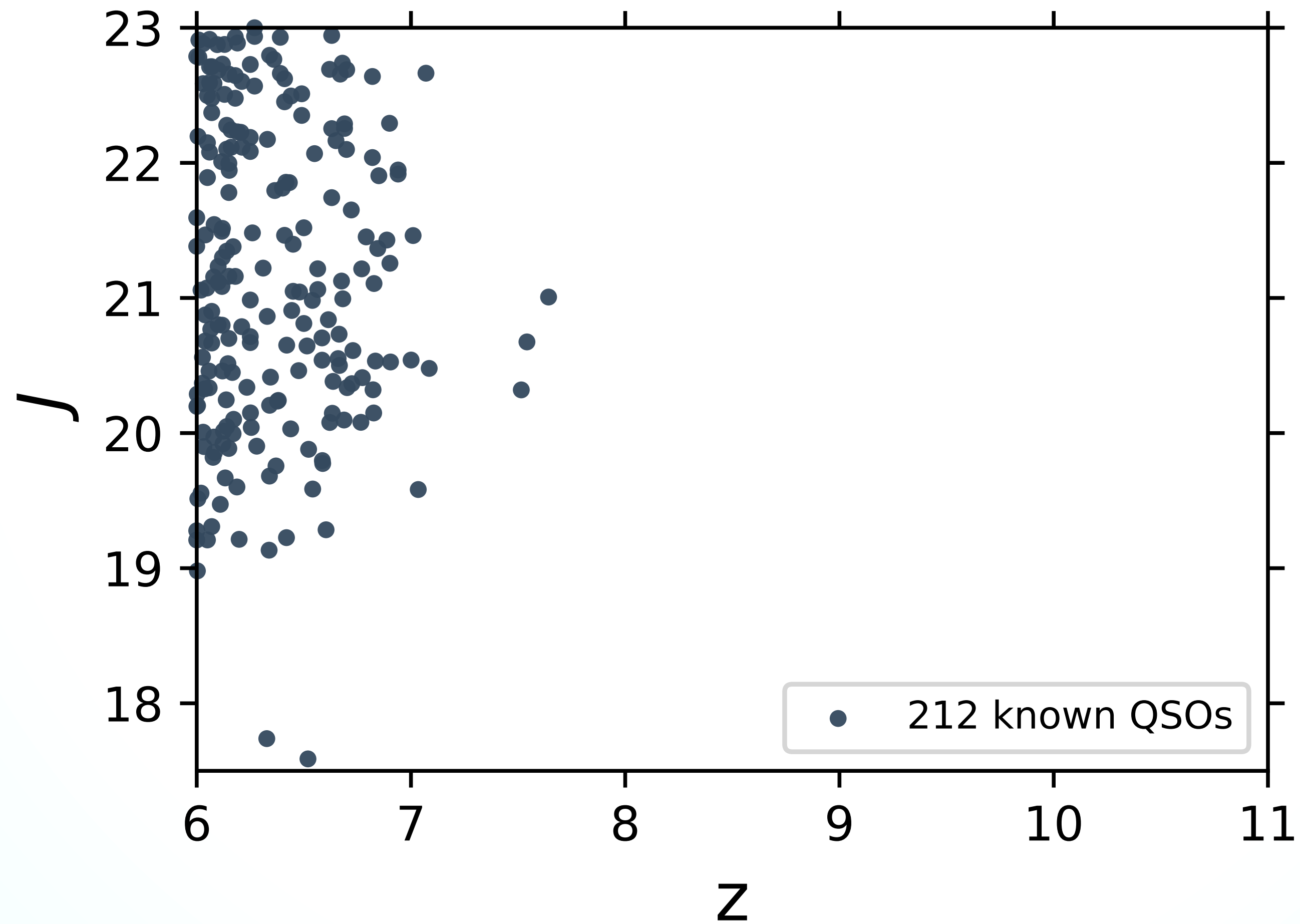


Lognormal t_Q distribution (Khrykin+ 2021)



EUCLID

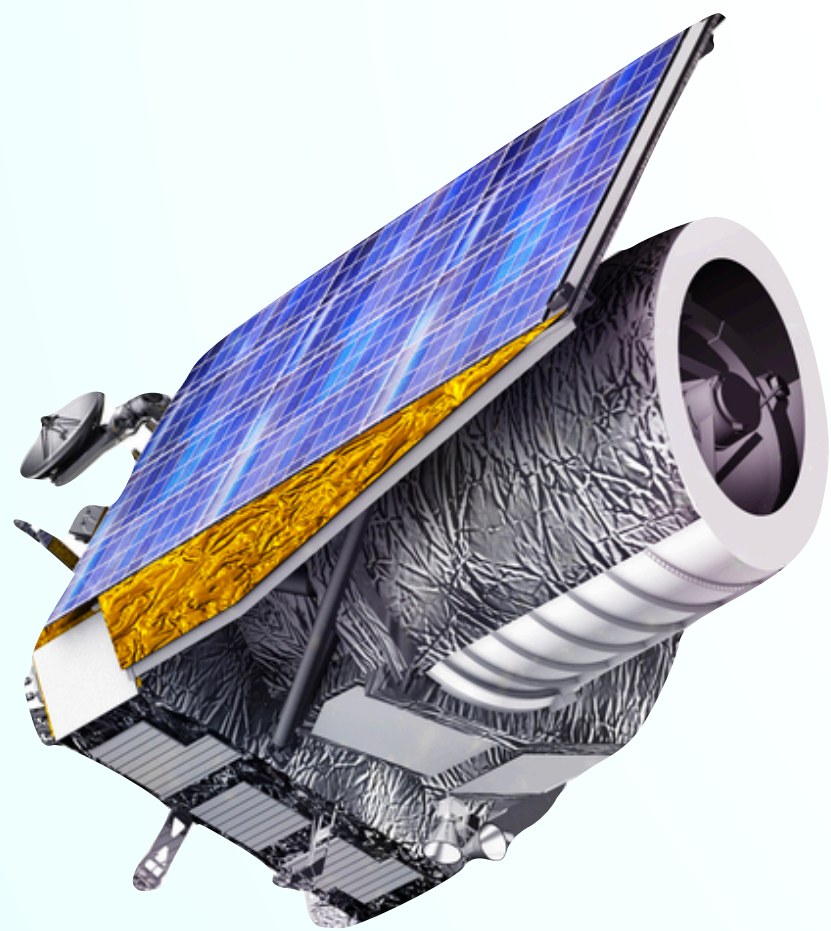
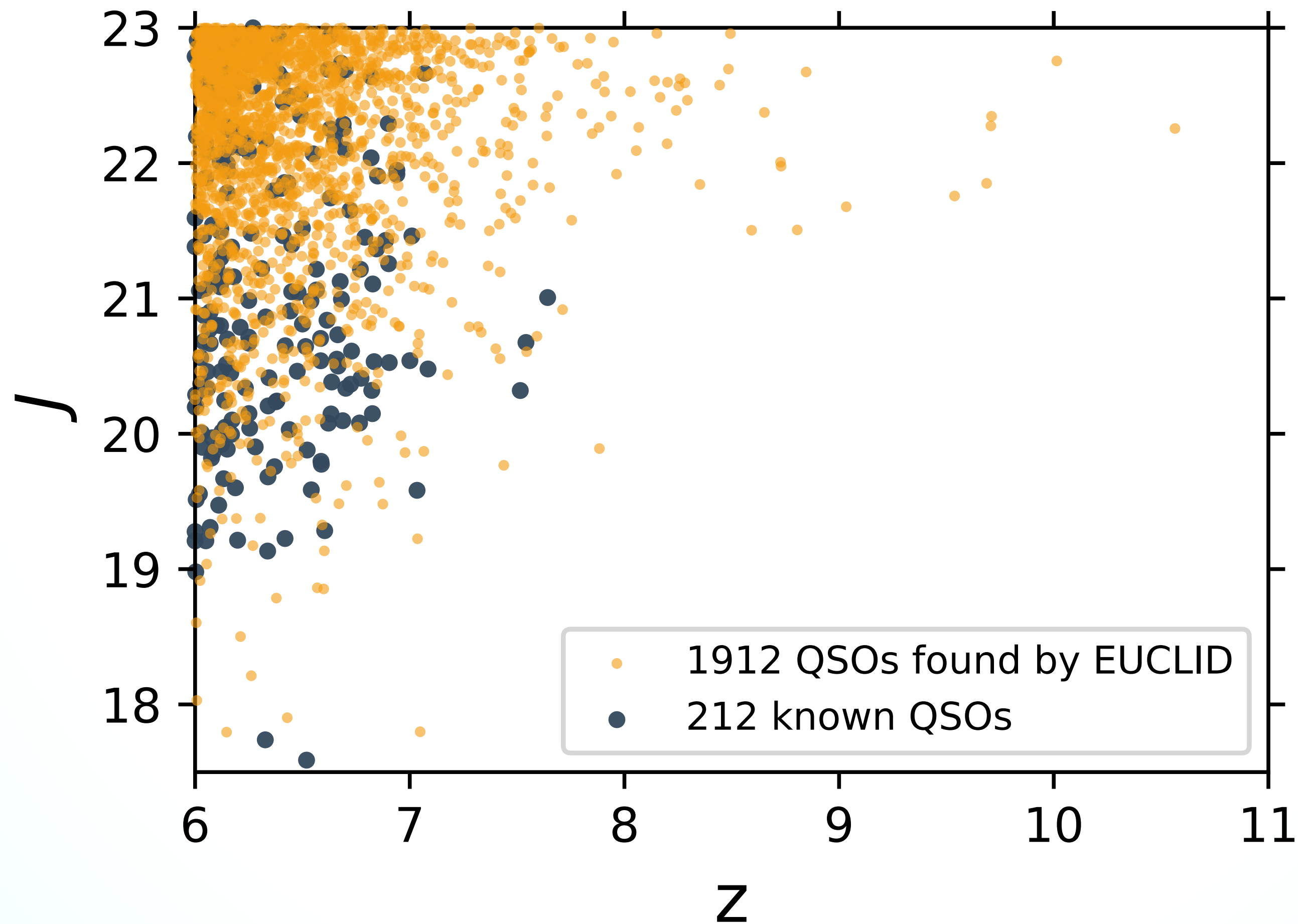
The Quasar Yield of the Wide-Field Survey



EUCLID

The Quasar Yield of the Wide-Field Survey

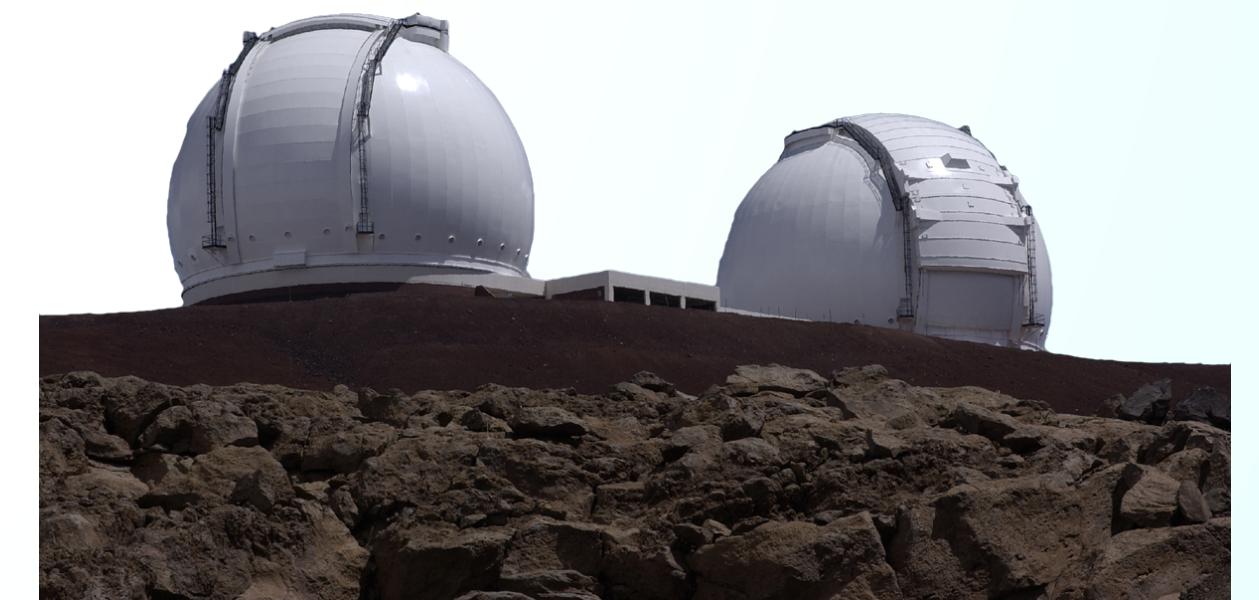
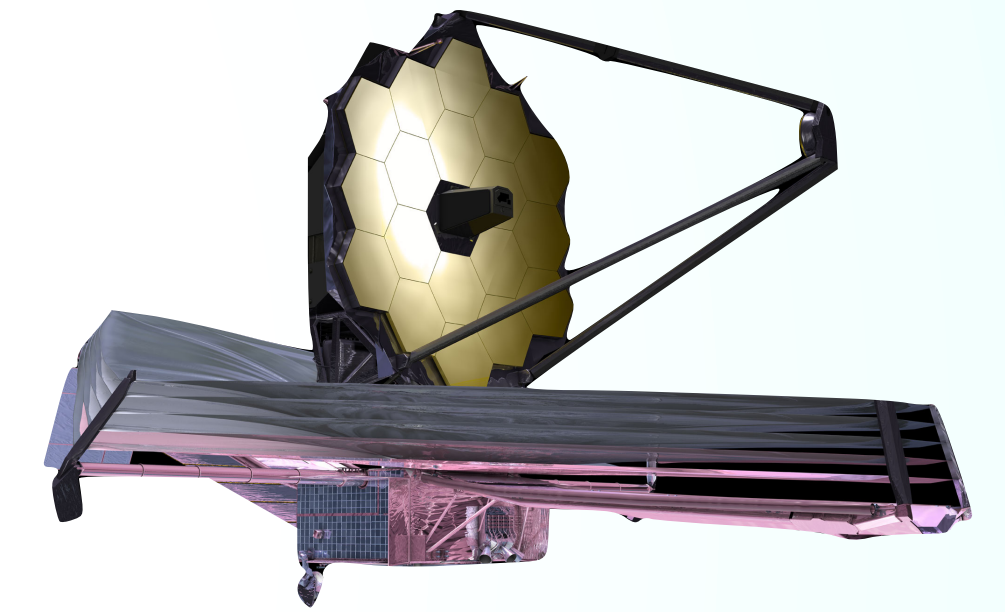
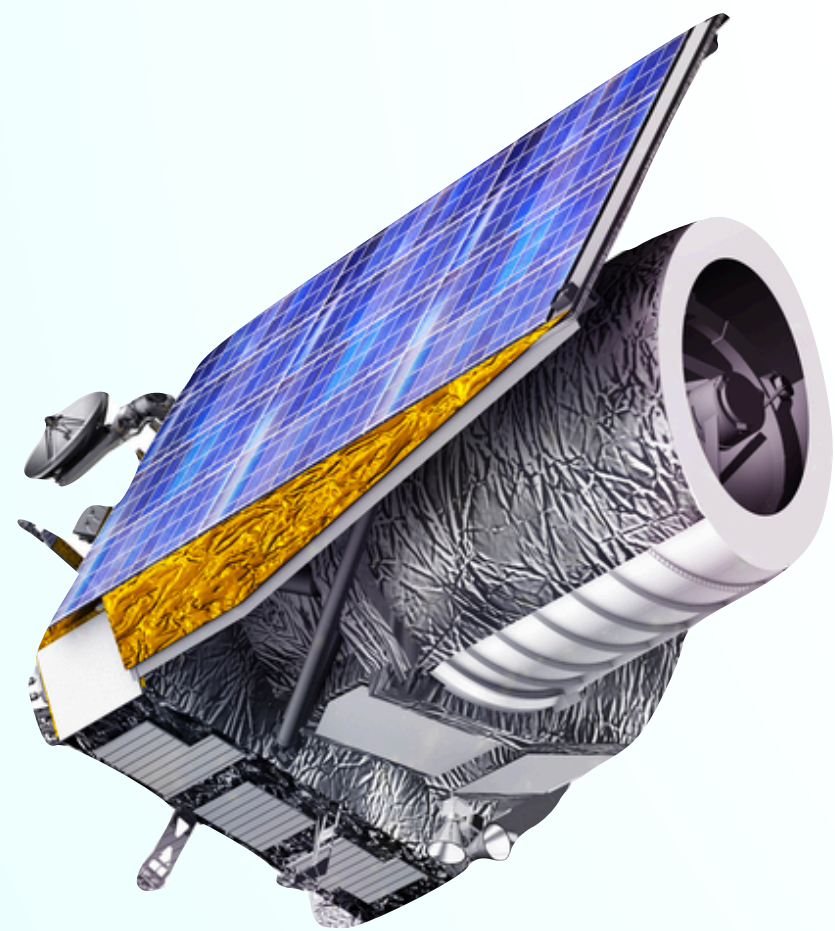
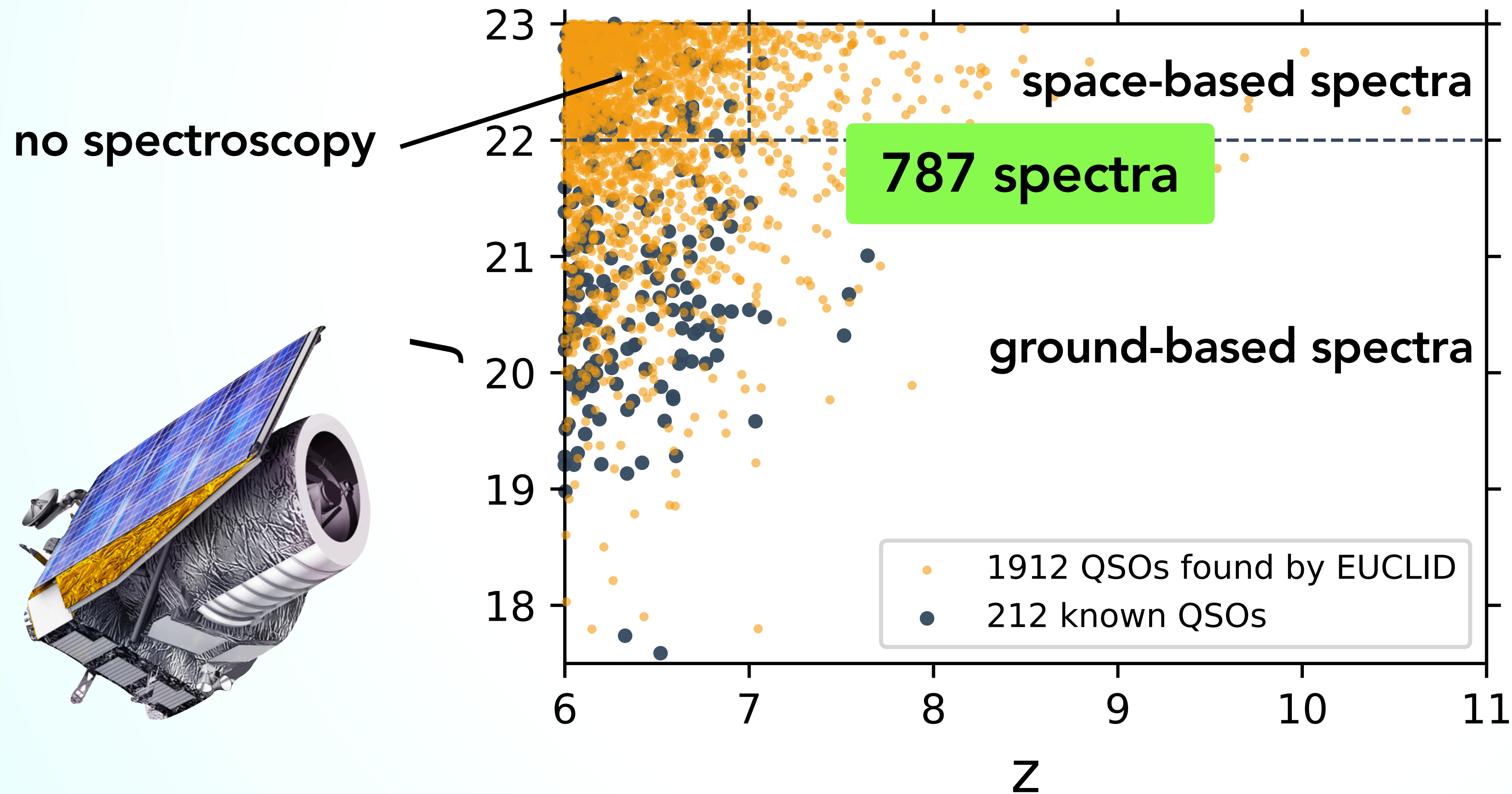
Samples from a Wang+2019 quasar luminosity function



EUCLID

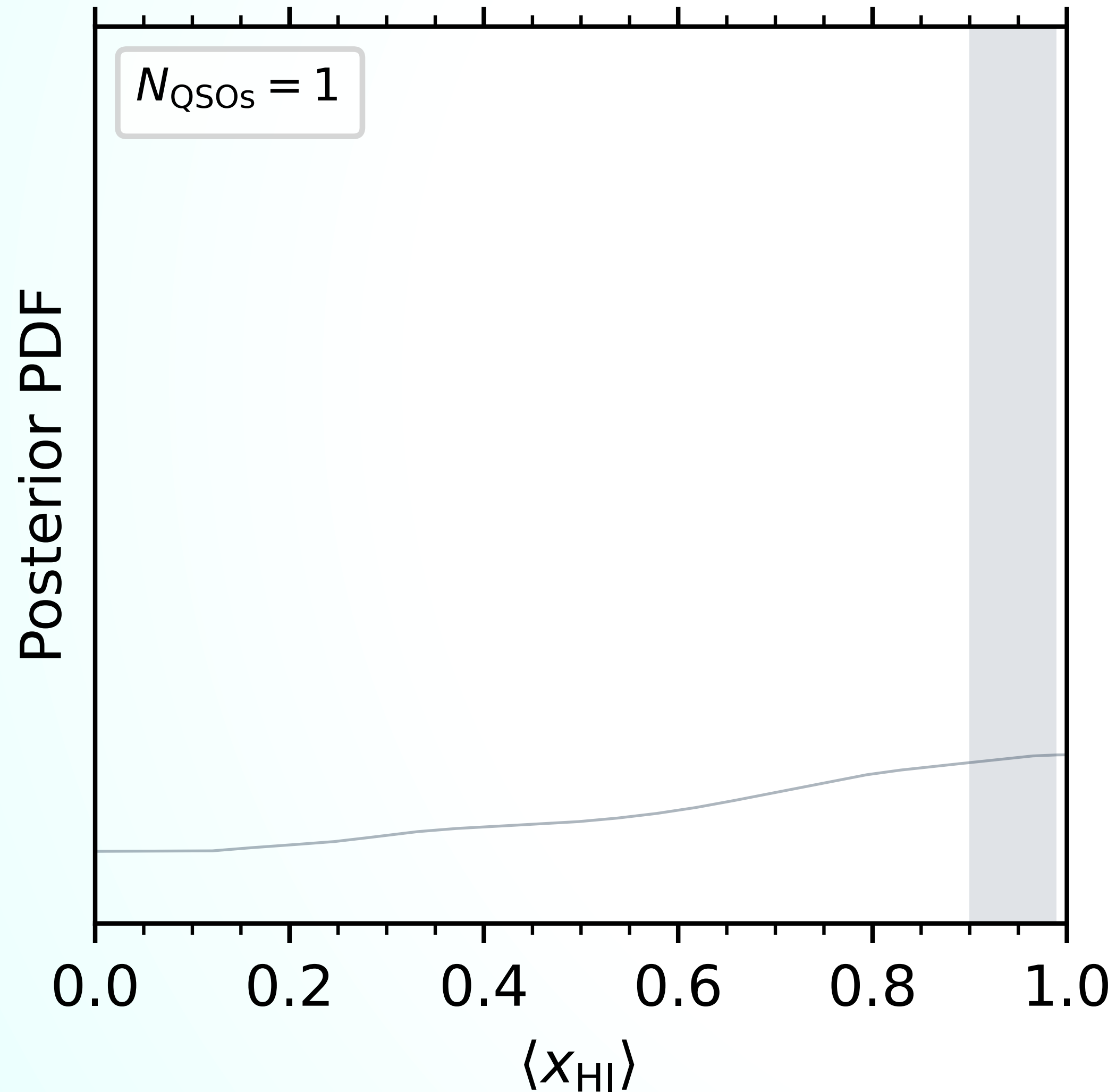
The Quasar Yield of the Wide-Field Survey

Samples from a Wang+2019 quasar luminosity function



Ensemble inference

Combining $\langle x_{\text{HI}} \rangle$ Posteriors

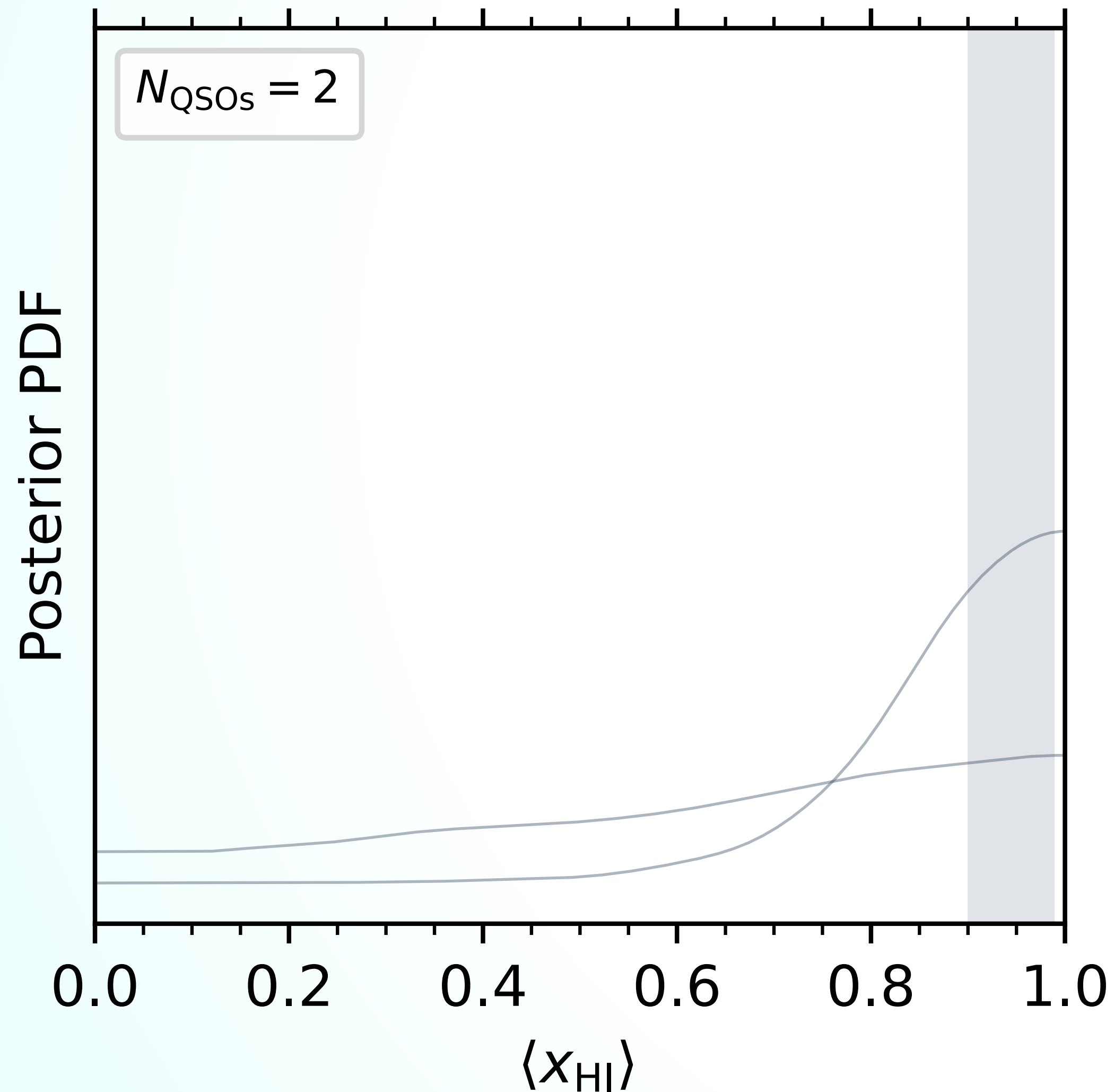


KDE of a single marginal $\langle x_{\text{HI}} \rangle$ -posterior inferred from a realistic mock observational spectrum:

- Full simulation model
- Latent PCA dimension 5
- Wavelength coverage up to 2000 Å, S/N = 10, FWHM = 100 km/s (rebinned to a 500 km/s pixel scale)

Ensemble inference

Combining $\langle x_{\text{HI}} \rangle$ Posteriors

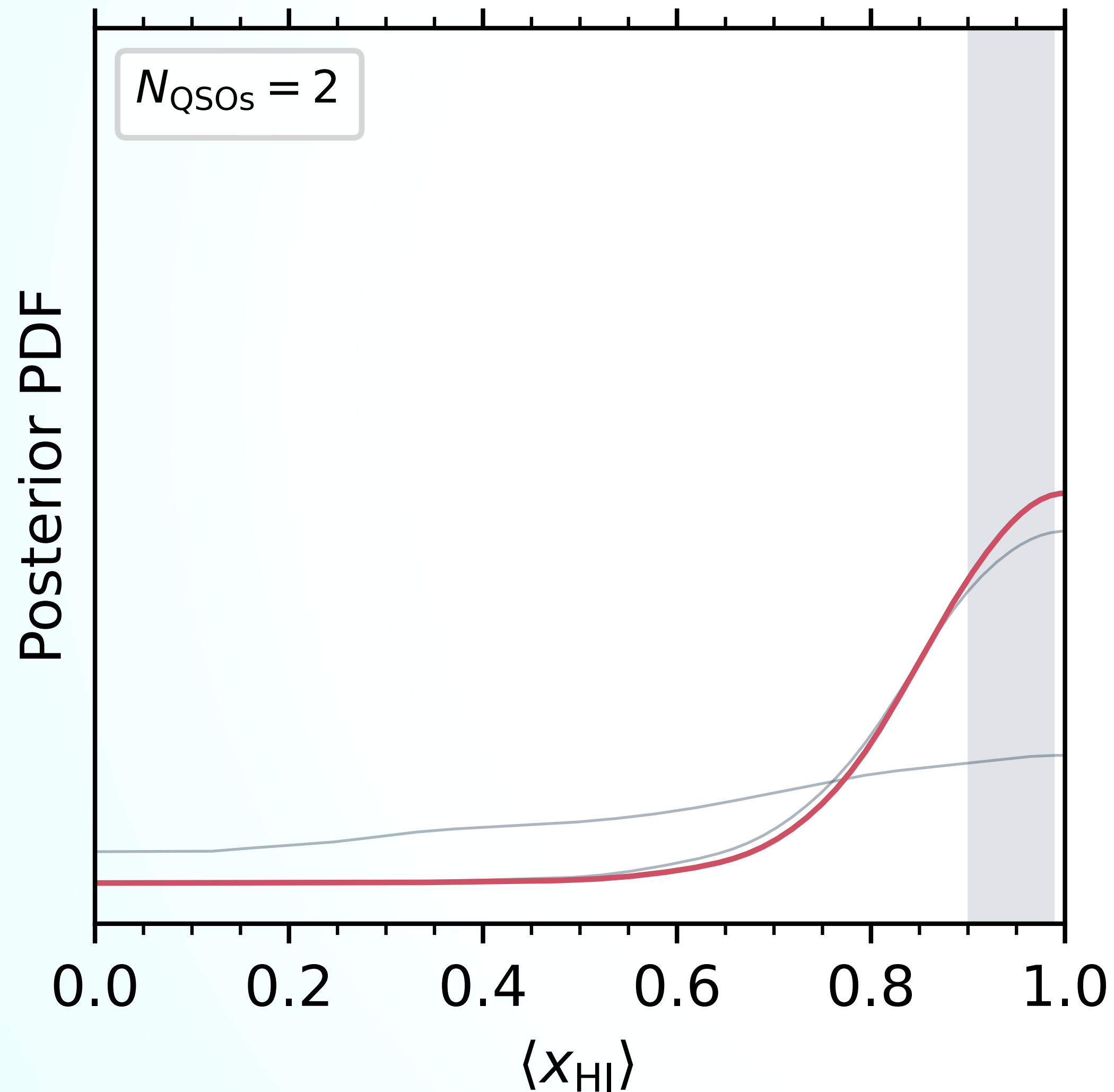


KDE of two marginal $\langle x_{\text{HI}} \rangle$ -posteriors inferred from realistic mock observational spectra:

- Full simulation model
- Latent PCA dimension 5
- Wavelength coverage up to 2000 Å, S/N = 10, FWHM = 100 km/s (rebinned to a 500 km/s pixel scale)

Ensemble inference

Combining $\langle x_{\text{HI}} \rangle$ Posteriors

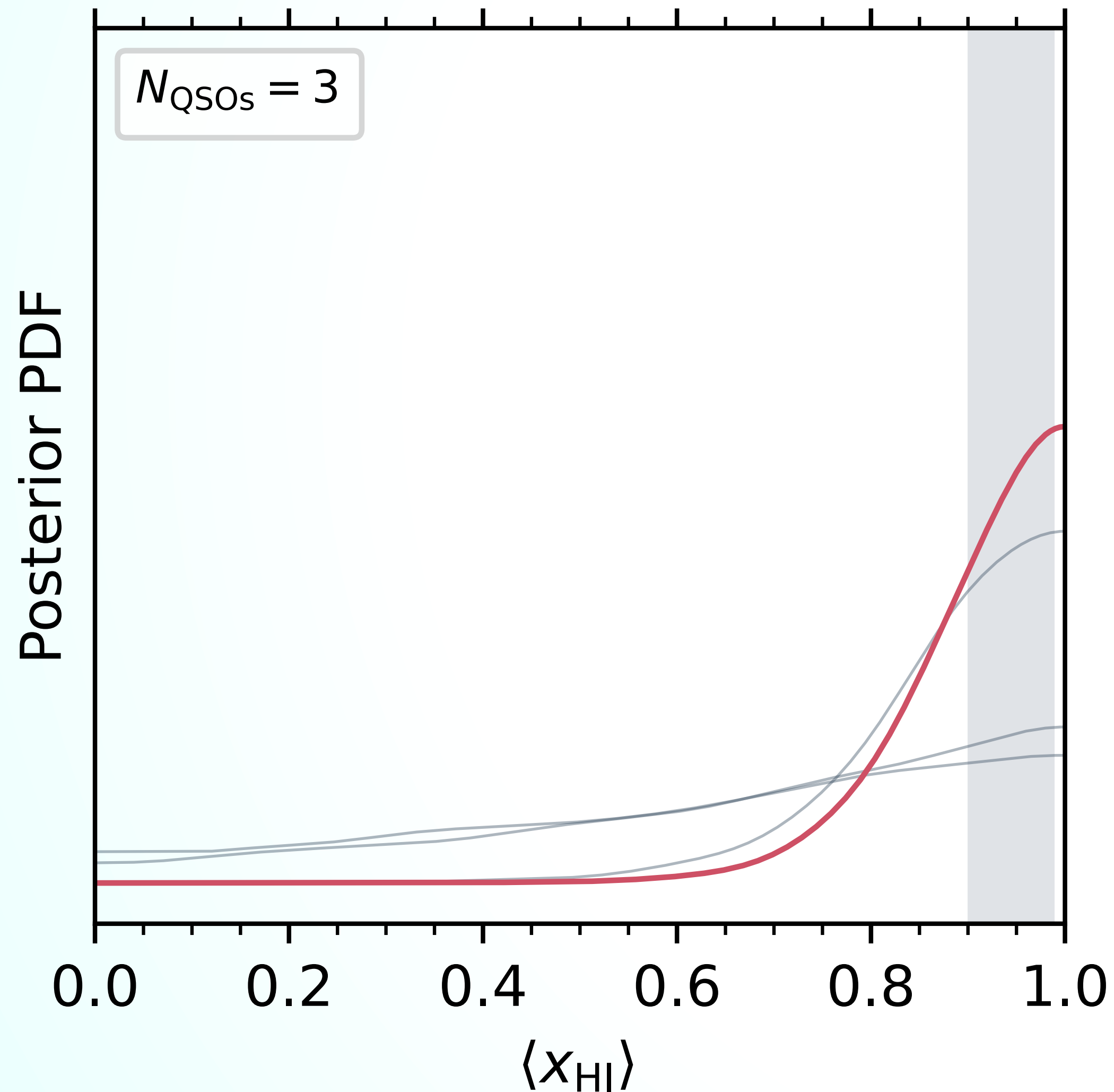


KDE of two marginal $\langle x_{\text{HI}} \rangle$ -posteriors inferred from realistic mock observational spectra:

- Full simulation model
- Latent PCA dimension 5
- Wavelength coverage up to 2000 Å, S/N = 10, FWHM = 100 km/s (rebinned to a 500 km/s pixel scale)

Ensemble inference

Combining $\langle x_{\text{HI}} \rangle$ Posteriors

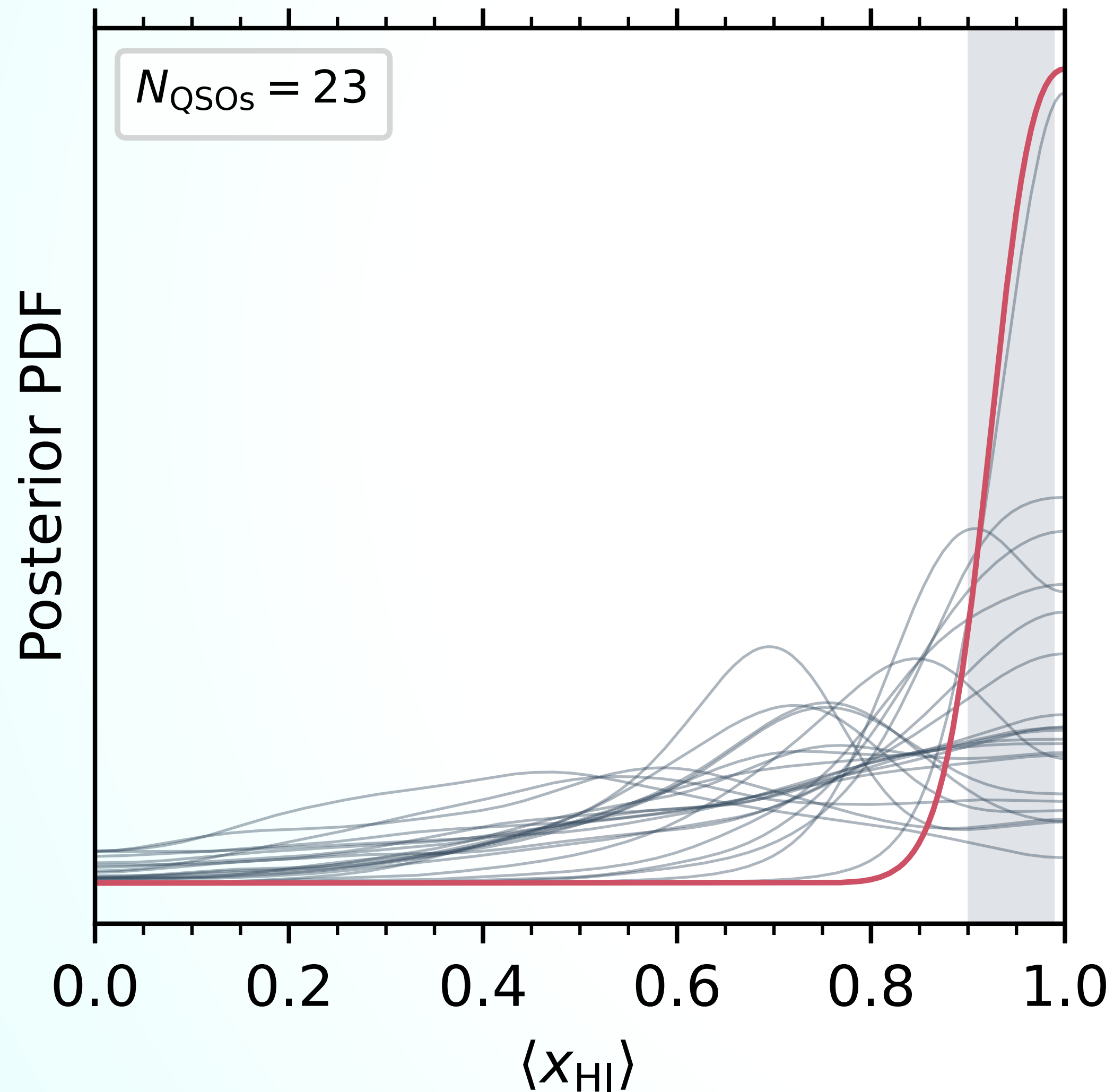


KDE of marginal $\langle x_{\text{HI}} \rangle$ -posteriors inferred from realistic mock observational spectra:

- Full simulation model
- Latent PCA dimension 5
- Wavelength coverage up to 2000 Å, S/N = 10, FWHM = 100 km/s (rebinned to a 500 km/s pixel scale)

Ensemble inference

Combining $\langle x_{\text{HI}} \rangle$ Posteriors

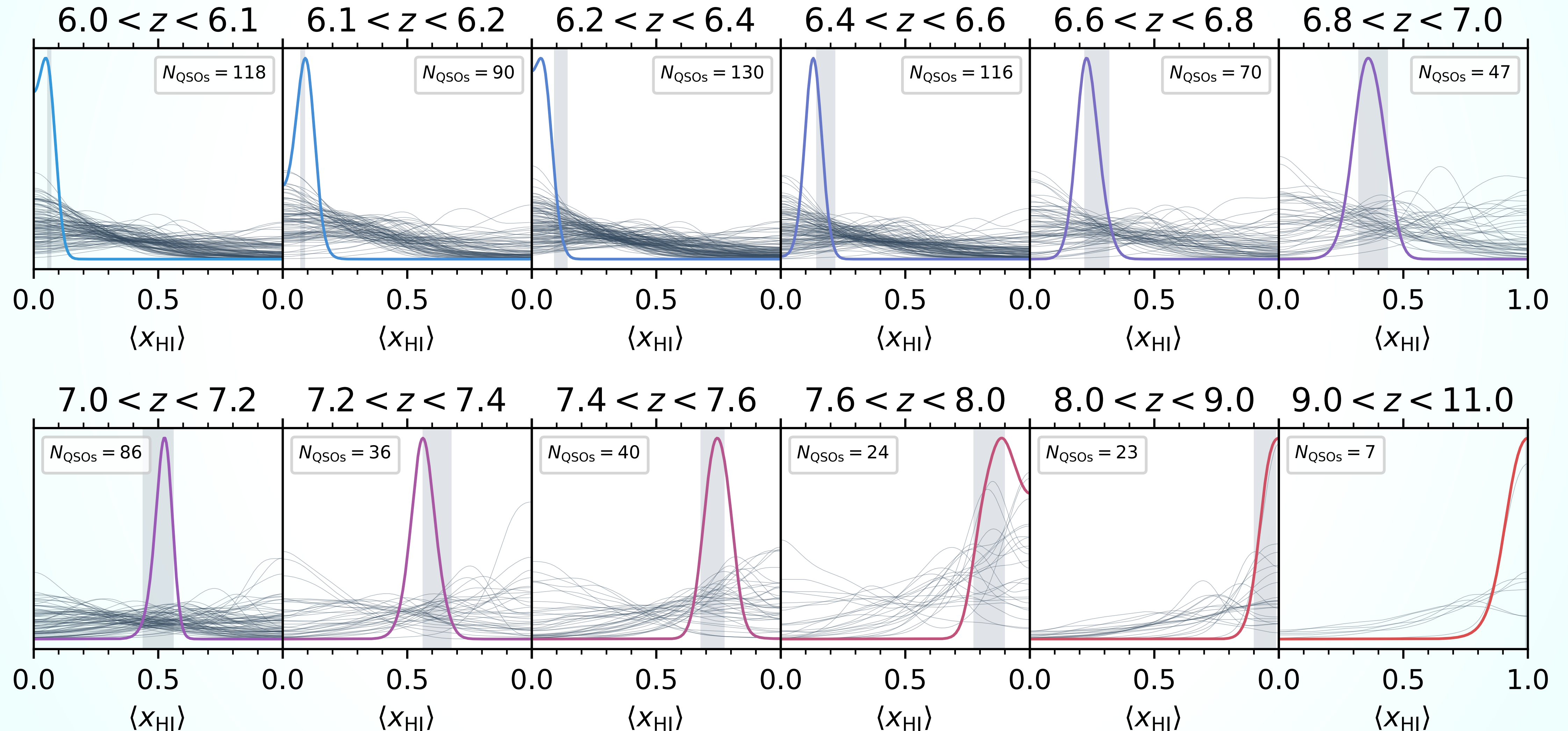


KDE of marginal $\langle x_{\text{HI}} \rangle$ -posteriors inferred from realistic mock observational spectra:

- Full simulation model
- Latent PCA dimension 5
- Wavelength coverage up to 2000 Å, S/N = 10, FWHM = 100 km/s (rebinned to a 500 km/s pixel scale)

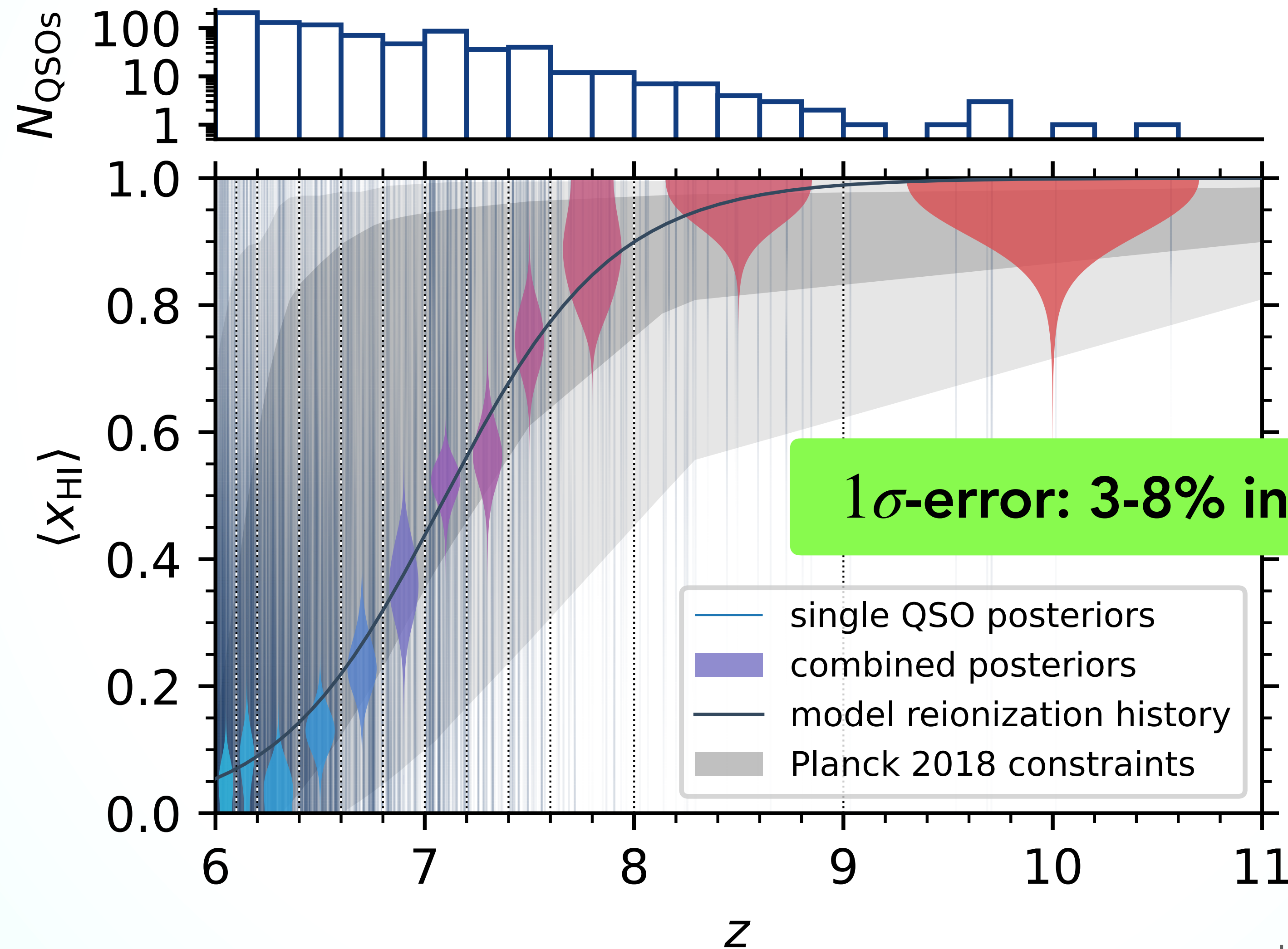
Ensemble inference

Constraining reionization history at the $\sim 5\%$ level with EUCLID & JWST

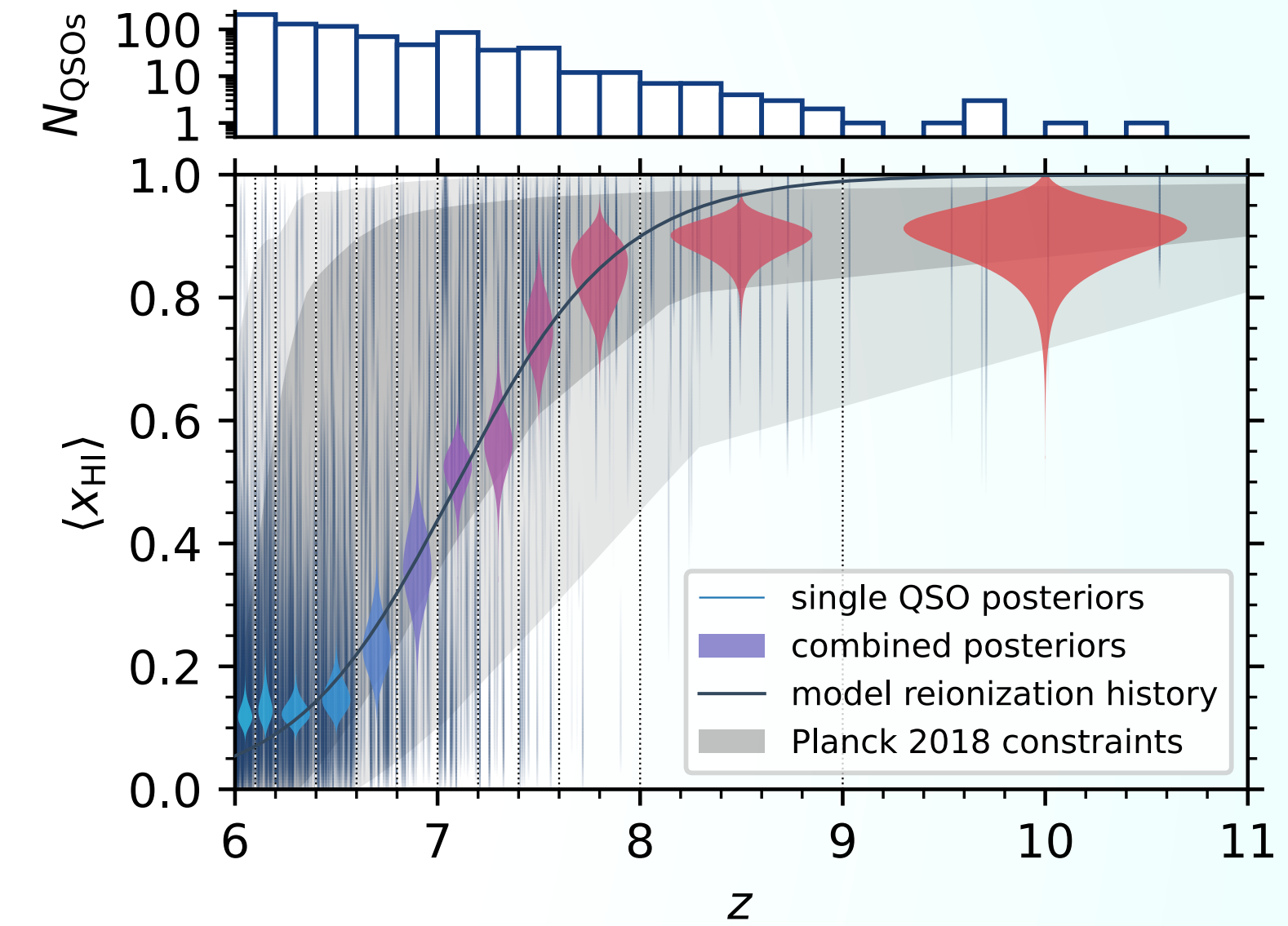
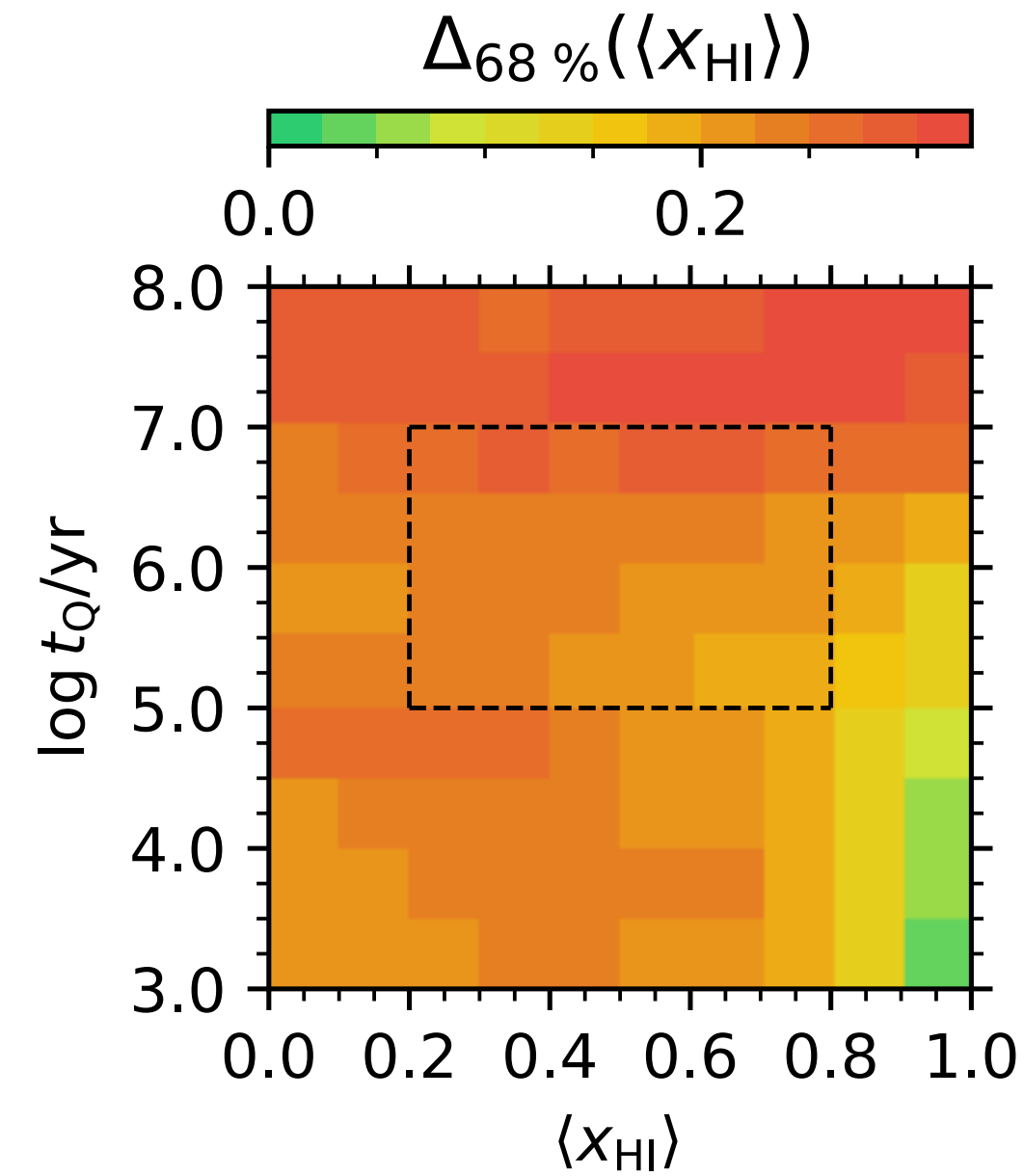
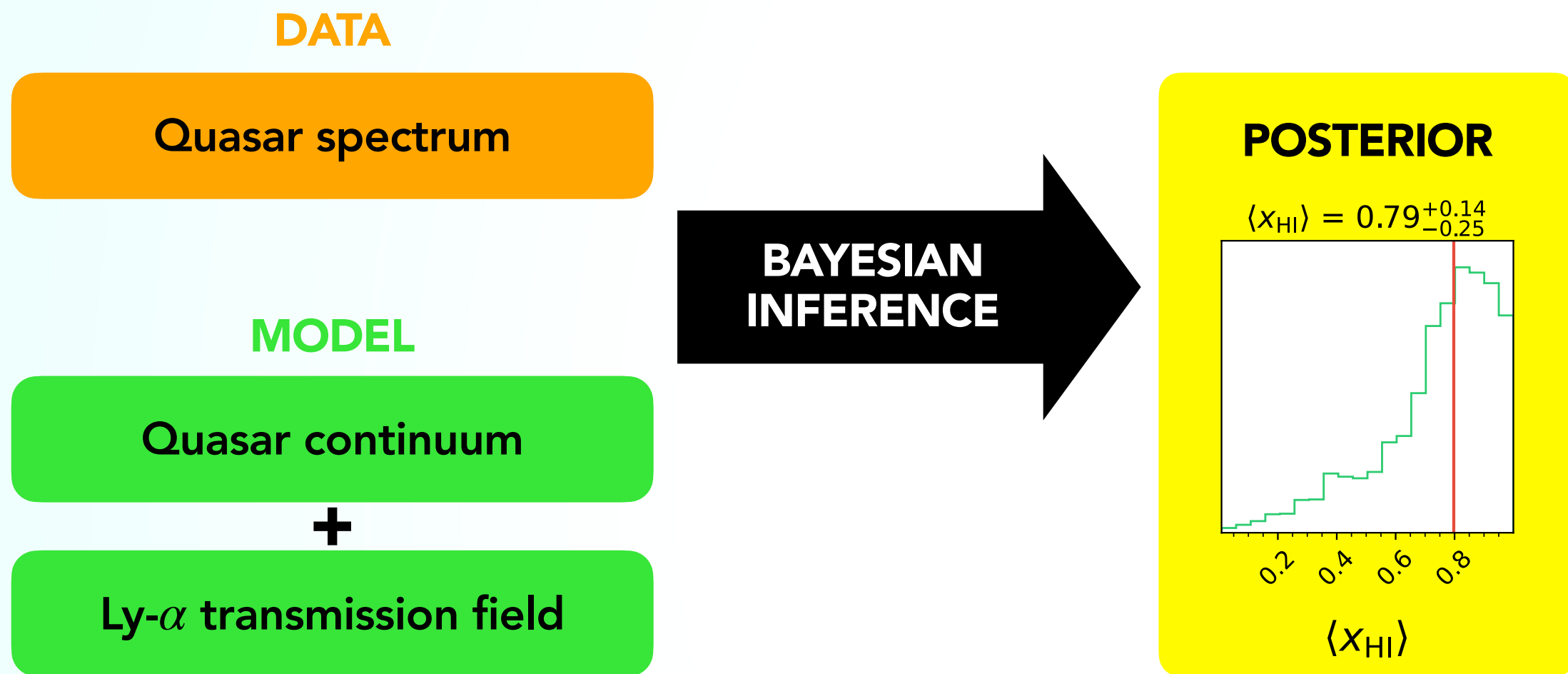


Ensemble inference

Constraining reionization history at the $\sim 5\%$ level with EUCLID & JWST



Summary



Fast Hamiltonian Monte-Carlo inference scheme to infer $\langle x_{\text{HI}} \rangle$ and t_{Q} using the damping wing signature of high-redshift quasars

Sensitivity analysis:
Apart from continuum reconstruction, stochasticity of reionization dominates the error budget

EUCLID forecast:
3-8% constraints on $\langle x_{\text{HI}} \rangle(z)$ throughout the Epoch of Reionization